STATE OF THE CALIFORNIA CURRENT 2013–14: EL NIÑO LOOMING

ANDREW W. LEISING,
ISAAC D. SCHROEDER,
STEVEN J. BOGRAD

Environmental Research Division
National Marine Fisheries Service
99 Pacific Street, Suite 255A
Monterey, CA 93940

ERIC P. BJORKSTEDT,
JOHN FIELD AND KEITH SAKUMA

Fisheries Ecology Division
National Marine Fisheries Service
110 Schaeffer Rd.
Santa Cruz, CA 95060

JEFFREY ABELL

Department of Oceanography
Humboldt State University

ROXANNE R. ROBERTSON

CIMEC, Humboldt State University

JOE TYBURCZY

California Sea Grant
Eureka, CA

WILLIAM T. PETERSON, RIC BRODEUR

Northwest Fisheries Science Center
National Marine Fisheries Service
Hatfield Marine Science Center
Newport, OR 97365

CAREN BARCELÓ

College of Earth, Ocean and
Atmospheric Sciences
Oregon State University
Corvallis, OR

TOBY D. AUTH[1]* AND
ELIZABETH A. DALY[2]

[1]Pacific States Marine Fisheries Commission
Hatfield Marine Science Center
2030 Marine Science Drive
Newport, Oregon 97365

[2]Cooperative Institute for
Marine Resources Studies
Oregon State University
Hatfield Marine Science Center
2030 Marine Science Drive
Newport, Oregon 97365

GREGORY S. CAMPBELL AND
JOHN A. HILDEBRAND

Scripps Institution of Oceanography
University of California, San Diego
9500 Gillman Drive
La Jolla, California 92093-0205

ROBERT M. SURYAN,
AMANDA J. GLADICS,
CHERYL A. HORTON,

Department of Fisheries and Wildlife
Oregon State University
Hatfield Marine Science Center
Newport, Oregon, 97365

MATI KAHRU[1] AND
MARLENNE MANZANO-SARABIA[2]

[1]Scripps Institution of Oceanography
University of California San Diego
La Jolla, CA 92121

[2]Facultad de Ciencias del Mar
Universidad Autónoma de Sinaloa
Mazatlán, Sinaloa, México

SAM MCCLATCHIE,
EDWARD D. WEBER, WILLIAM WATSON

NMFS, Southwest Fisheries Science Center
8901 La Jolla Shores Drive
La Jolla, CA 92037-1508

JARROD A. SANTORA
AND WILLIAM J. SYDEMAN

Farallon Institute for
Advanced Ecosystem Research
101 H St.
Petaluma, CA 94952

SHARON R. MELIN AND
ROBERT L. DELONG

National Marine Fisheries Service
Alaska Fisheries Science Center
National Marine Mammal Laboratory, NOAA
7600 Sand Point Way N. E.
Seattle, WA 98115

JOHN LARGIER

Bodega Marine Laboratory
University of California, Davis
P.O. Box 247
Bodega Bay, CA 94923

SUNG YONG KIM

Division of Ocean Systems Engineering
Korea Advanced Institute of
Science and Technology
Yuseong-gu, Daejeon 305-701
Republic of Korea

FRANCISCO P. CHAVEZ

Monterey Bay Aquarium Research Institute
7700 Sandholdt Road
Moss Landing, CA 95039

RICHARD T. GOLIGHTLY,
STEPHANIE R. SCHNEIDER

Department of Wildlife
Humboldt State University
1 Harpst Street
Arcata, CA 95521

PETE WARZYBOK,
RUSSEL BRADLEY, JAIME JAHNCKE

Point Blue Conservation Science
(formerly PRBO)
3820 Cypress Drive, Suite 11
Petaluma, CA 94954

JENNIFER FISHER AND
JAY PETERSON

Oregon State University
Cooperative Institute for
Marine Resources Studies
Hatfield Science Center
Newport, OR

ABSTRACT

In 2013, the California current was dominated by strong coastal upwelling and high productivity. Indices of total cumulative upwelling for particular coastal locations reached some of the highest values on record. Chlorophyll *a* levels were high throughout spring and summer. Catches of upwelling-related fish species were also high. After a moderate drop in upwelling during fall 2013, the California current system underwent a major change in phase. Three major basin-scale indicators, the PDO, the NPGO, and the ENSO-MEI, all changed phase at some point during the winter of 2013/14. The PDO changed to positive values, indicative of warmer waters in the North Pacific; the NPGO to negative values, indicative of lower productivity along the coast; and the MEI to positive values, indicative of an oncoming El Niño. Whereas the majority of the California Current system appears to have transitioned to an El Niño state by August 2014, based on decreases in upwelling and chlorophyll *a* concentration, and increases in SST, there still remained pockets of moderate upwelling, cold water, and high chlorophyll *a* biomass at various

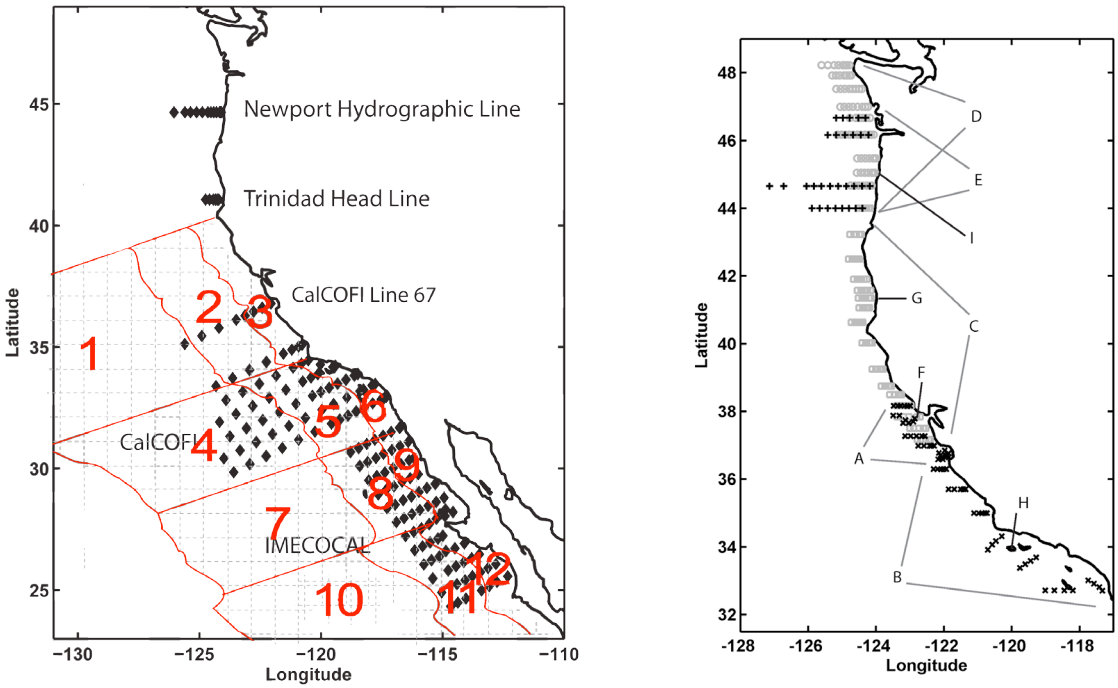

Figure 1. Left: Station maps for surveys that were conducted multiple times per year during different seasons to provide year-round observations in the California Current system. The CalCOFI survey (including CalCOFI Line 67) was occupied quarterly; the spring CalCOFI survey grid extends just north of San Francisco. The IMECOCAL survey is conducted quarterly or semiannually, however, there was no sampling during 2013 due to a changeover in vessels during that year. The Newport Hydrographic Line was occupied biweekly. The Trinidad Head Line was occupied at biweekly to monthly intervals. Right: Location of annual or seasonal surveys, including locations of studies on higher trophic levels, from which data was included in this report. Different symbols are used to help differentiate the extent of overlapping surveys. Red overlay and numbers denotes areas for SST and chlorophyll *a* analysis. A. SWFSC Fisheries Ecology Division (FED) midwater trawl survey core region (May–June) B. SWFSC FED midwater trawl survey south region (May–June). C. SWFSC FED salmon survey (June and September) (grey squares). D. NWFSC salmon survey (May, June, and September). E. NOAA/BPA pelagic rope trawl survey (May through September). F. Southeast Farallon Island. G. Castle Rock. H. San Miguel Island. I. Yaquina Head Outstanding Natural Area.

central coast locations, unlike patterns seen during the more major El Niños (e.g., the 97–98 event). Catches of rockfish, market squid, euphausiids, and juvenile sanddab remained high along the central coast, whereas catches of sardine and anchovy were low throughout the CCS. 2014 appears to be heading towards a moderate El Niño state, with some remaining patchy regions of upwelling-driven productivity along the coast. Superimposed on this pattern, three major regions have experienced possibly non-El Niño-related warming since winter: the Bering Sea, the Gulf of Alaska, and offshore of southern California. It is unclear how this warming may interact with the predicted El Niño, but the result will likely be reduced growth or reproduction for many key fisheries species.

INTRODUCTION

This report reviews the oceanographic and ecosystem responses of the California Current system (CCS) between spring 2013 and spring of 2014. Biological and hydrographic data from a number of academic, private, and government institutions have been consolidated and described in the context of historical data (fig. 1). The various institutions have provided data and explanation of the data after an open solicitation for contributions; these contributions are acknowledged in the author list. These data are synthesized here, in the spirit of providing a broader description of the present condition of the CCS. All data are distilled from complex sampling programs covering multiple spatial and temporal scales into simple figures that may not convey the full complexity of the region being studied. As a consequence, we focus on the findings of the data and limit our descriptions of the methodology to only that which is required for interpretation. More complete descriptions of the data and methodologies can be found through links to the individual survey programs. The survey designs that we examine are dissimilar and each has unique limitations restricting a common interpretation within the California Current Large Marine Ecosystem (CCLME). Therefore, this report should be considered a first examination for instigating more focused exploration of potential drivers of the ecosystem dynamics.

This report will focus on data highlighting the conditions during 2013–spring 2014, with a particular emphasis on the evidence that the CCS may be transitioning to El Niño conditions during 2014. New for the report this year, we have moved some of the physical supporting data from this document to an online supplement (http://www.calcofi.org/ccpublications/ccreports/state-

TABLE 1
List of CCS indices, their current status, and link to live supplement (e.g., S1 = supplement Figure 1).

Index	Current State	Trend	Implication	Link
PDO	Positive	Increasing	Warming	S1
NPGO	Negative	Decreasing	Low Productivity	S1
ENSO (MEI)	Positive	Increasing	El Niño	S1
Upwelling Anomaly	Negative	Neutral	Warm, low productivity	Fig. 2, S2
Cumulative Upwelling	Neutral	Neutral	Average yearly upwelling	Fig. 3, S3
SST Anomaly	Positive	Increasing	Warm surface waters	Fig. 4, 7, S4, S5
Wind Anomaly	Cyclonic	Anti- to Cyclonic	Warm surface waters	Fig. 4, S5
Temperature-Salinity, CalCOFI	Warmer and Saltier at N Coastal, Surface	NA	Change in transport	S6
Mixed-Layer Salinity, CalCOFI	Positive Anomaly	Decreasing	NA	S7
Mixed-Layer NO3, CalCOFI	Negative Anomaly	Neutral	Decreased Productivity	S7
Nitricline Depth, CalCOFI	Negative Anomaly	Decreasing	Decreased productivity	S7
Integrated chlorophyll *a*, CalCOFI	Neutral	Neutral	Similar to long-term mean	S8
Integrated PP, CalCOFI	Positive Anomaly	Increasing	Possibly higher productivity	S8
Zooplankton Volume, CalCOFI	Positive Anomaly	Increasing	Increased secondary production	S8
Chlorophyll *a* Profiles, CalCOFI	High in Coastal North	NA	Increased productivity	S9
Chlorophyll *a*	Negative	Decreasing	Low productivity	S10

of-the-current.html). The goal is to create a "live" State of the California Current (SOTCC) web page resource, where information can be rapidly obtained as to the most recent, up-to-date state of the CCS. As a result, several long-term time series of physical climate that have traditionally been found within this document have been replaced by a table stating only their current state, along with a link to the appropriate web page. As in past reports, we begin with an analysis of large-scale climate modes and upwelling conditions in the California Current. Following, the various observational data sampling programs are reviewed to highlight the links between ecosystem structure, processes, and climate. Lastly, a short synthesis/discussion of the most recent conditions within the CCS and the potential implications of the looming El Niño are presented.

NORTH PACIFIC CLIMATE INDICES

The winter of 2013–14 marked a transition of a cool phase in the North Pacific as indicated by the Pacific Decadal Oscillation index (table 1, PDO; Mantua and Hare 2002) and strong California Current strength with associated high nutrient levels as indicated by the North Pacific Gyre Oscillation (table 1, NPGO; Di Lorenzo et al. 2008) index. The PDO switched to positive values in January 2014 after four years of continuous negative values, while the NPGO switched to negative values in October 2013 after seven years of continuous positive values (online supplement, fig. S1). These transitions are likely due to variations in the strength of the Aleutian Low pressure system in the winter, which is highly influenced by the onset of El Niño events (Bjerknes 1966; Trenberth and Hurrell 1994). The multivariate El Niño Southern Oscillation (ENSO) index (MEI; Wolter and Timlin 1998) transitioned from neutral La Niña conditions in 2013 to positive values in April 2014. The April value (0.93) of the MEI was slightly less than the maximum value experienced in the short-lived El Niño event in the winter of 2010 (MEI value of 1.5 for February 2010) (fig. 2). The NINO3.4 index (which is the SST anomalies averaged over 5°S–5°N and 120°W–170°W; http://www.cpc.ncep.noaa.gov/data/indices/wksst8110.for) indicated El Niño conditions, as values greater than 0.5°C were reached during May 2014 with an anomaly of 0.6°C. The September NINO3.4 values were just at the threshold indicating an El Niño event and were much lower than the anomalies at the height of the 1997–98 El Niño event, which had anomalies over 2.5°C. However, short-term forecasts suggest that a weak El Niño event may be imminent (http://www.cpc.ncep.noaa.gov/products/analysis_monitoring/enso_advisory/ensodisc.html).

Upwelling in the California Current

Monthly means of daily upwelling index (Bakun 1973; Schwing et al. 1996) indicated downwelling conditions from October to December of 2012 for areas north of 33°N. The downwelling quickly switched to strong upwelling (values >50 $m^3\ s^{-1}$ per 100 m) in January 2013 (fig. 2). The anomalies of the upwelling index showed strong upwelling relative to long-term means (anomaly values >50 $m^3\ s^{-1}$ per 100 m) during 2013 especially in January, April, July and December for latitudes between 36° and 48°N. The positive upwelling anomalies (calculated form monthly means for 1967–2013) continued into January 2014, but since February 2014 upwelling has been near the climatological mean. The cumulative upwelling index (CUI) provides an estimate of the net influence of upwelling on ecosystem structure and productivity over the course of the year (Bograd et al. 2009). For all latitudes the CUI for 2013 was one of the highest over the past 40 years and was

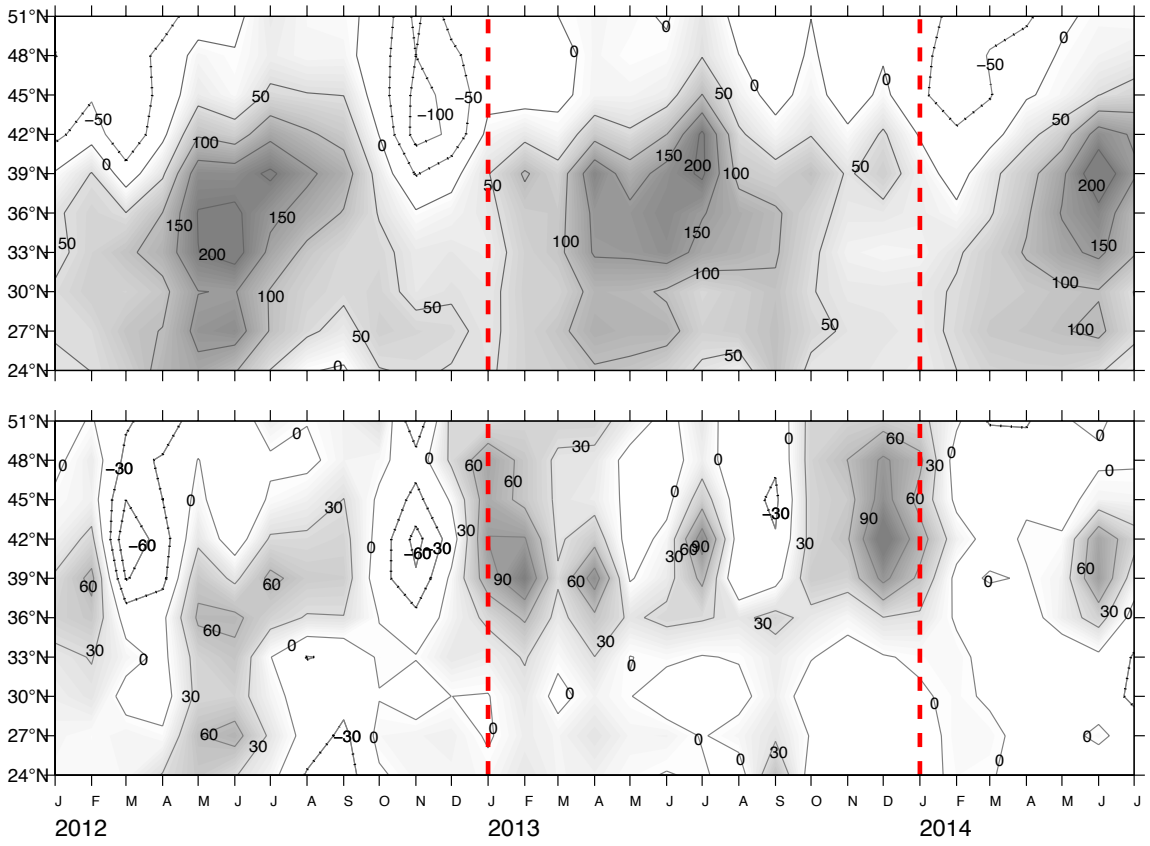

Figure 2. Monthly means of daily Bakun Upwelling Index (top) and anomalies (bottom) for January 2012–July 2014. Shaded areas denote positive (upwelling-favorable) values in upper panel, and positive anomalies (generally greater than normal upwelling) in lower panel. Anomalies are relative to 1967–2013 monthly means. Units are in $m^3\ s^{-1}$ per 100 m of coastline. Daily upwelling index data obtained from http://pfeg.noaa.gov/products/PFELData/upwell/daily.

the highest on record for latitudes 39°–48°N (fig. 3). In 2014 the CUI was high during mid to late January, especially for the northernmost latitudes, but soon dropped towards the long-term mean by the end of May.

North Pacific Climate Patterns

A basin-scale examination of SST allows for the interpretation of the spatial evolution of climate patterns and wind forcing over the North Pacific related to trends in the basin-scale and upwelling indices (figs. 2, 3). In the summer of 2013, predominantly positive SST anomalies (calculated from a climatology based on 1950–79) less than 0.5°C extended over most of the North Pacific, with the highest anomalies of 1°C occurring in the Northeast Pacific (fig. 4). These high temperatures were concurrent with anticyclonic wind anomalies which result in increased alongshore upwelling producing winds and negative SST anomalies along the Oregon and Washington coast. The same pattern extended into December 2013 with increased SST (> +2.0°C) anomalies in the Northeast Pacific with increased anticyclonic wind anomalies, resulting in strong upwelling along the US West Coast and negative SST (–1.0°C) anomalies. In February 2014, these high SST anomalies persisted while the area of highest anticyclonic wind anomalies dropped from ~40°N in July and December of 2013 to ~30°N. The wind anomalies for February 2014 (calculated from a climatology based on 1968–96) also show a cyclonic pattern in the northeast Pacific due to a deepening of the Aleutian Low pressure system. In May 2014, positive SST anomalies (>1.0°C) extended across the Equatorial Pacific and along the West Coast of North America from Alaska to Mexico, with the exception of a narrow band of coastal waters (within 60 miles offshore) off of central and northern California, where strong upwelling winds kept the ocean cool and productive thorough May and June of 2014 (not shown in fig. 4).

Coastal Sea Surface Temperature

In 2013, the daily January through April SST, as measured by National Data Buoy Center (NDBC) buoys, were lower than the climatological mean (based on the total time series for each individual buoy; see: http://www.ndbc.noaa.gov for specific details) for all buoys along the West Coast from Oregon (northernmost location 46050: 44.639 N 124.534 W) to south-

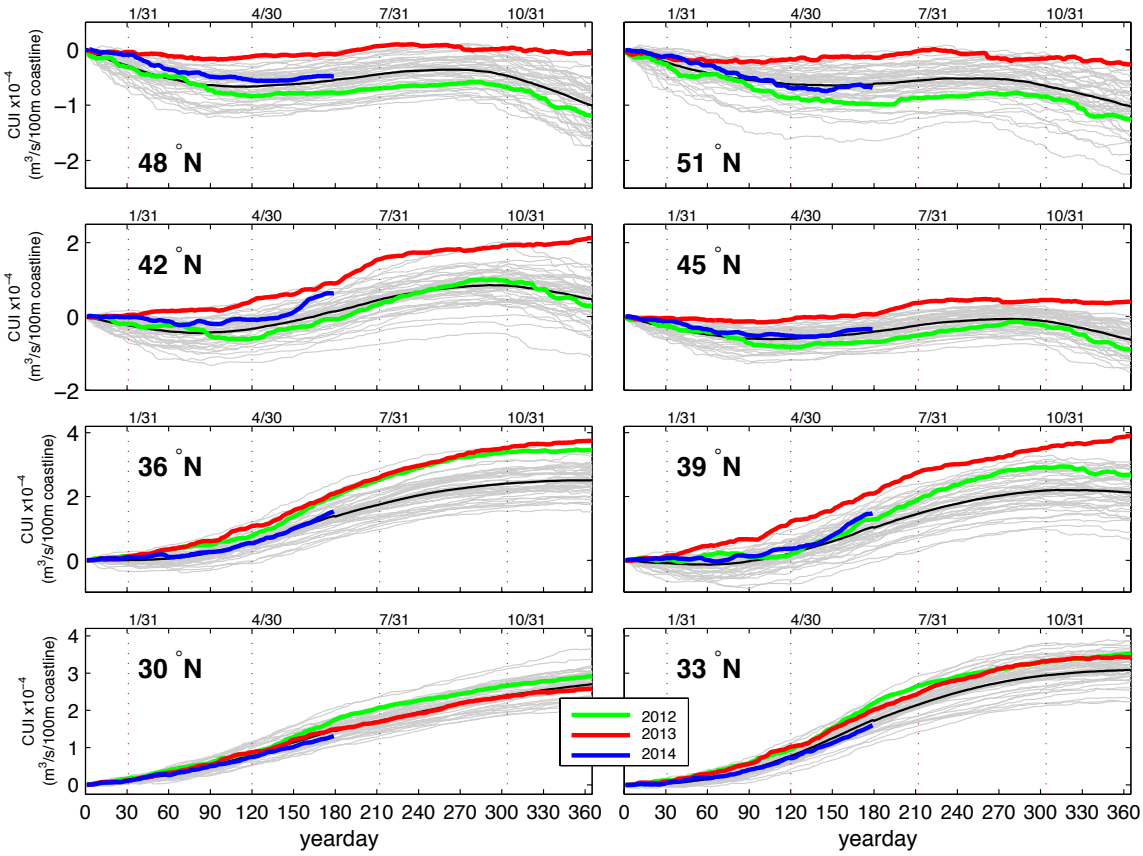

Figure 3. Cumulative upwelling index (CUI) from January 1 calculated from the daily Bakun Upwelling Index at locations along the West Coast of North America for 1967–2013 (grey lines), the mean value for the period 1967–2011 (black line), 2012 (green line), 2013 (red line), and 2014 (blue line). The red dashed vertical lines mark the end of January, April, July and October.

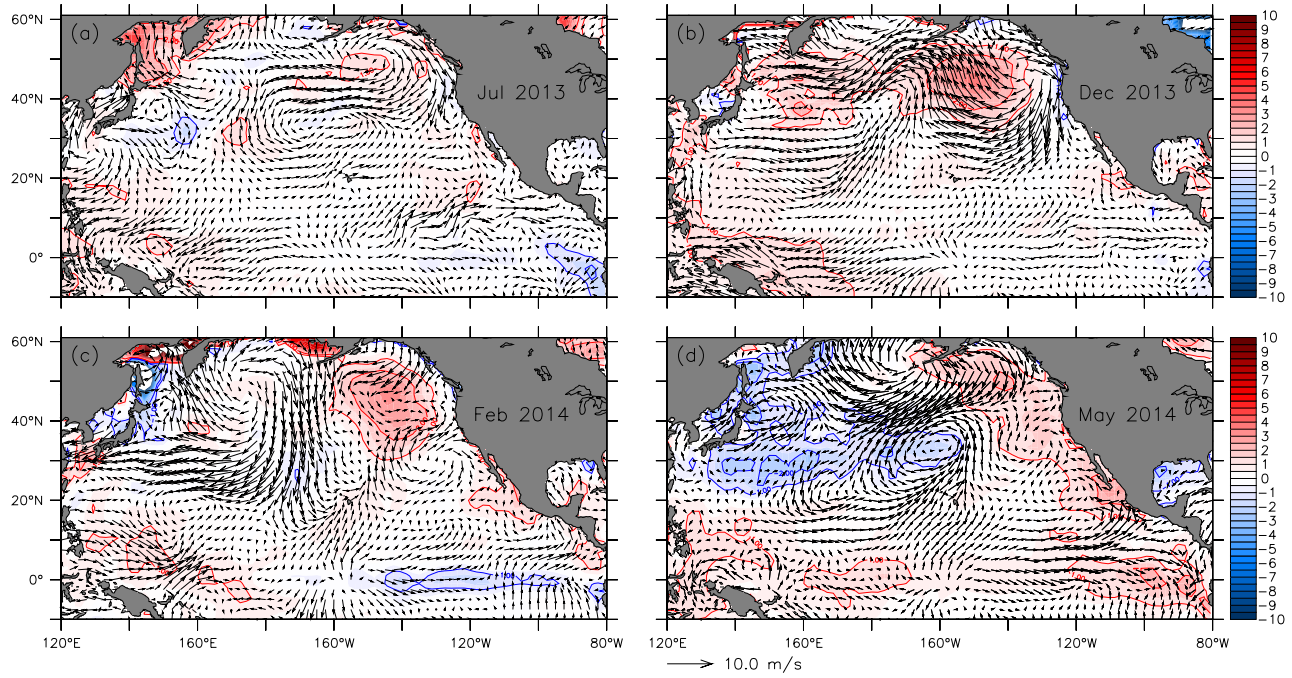

Figure 4. Anomalies of surface wind velocity and sea surface temperature (SST) in the North Pacific Ocean, July 2013, December 2013, February 2014, and May 2014. Arrows denote magnitude and direction of wind anomaly (scale arrow at bottom). Contours demote SST anomaly. Shading interval is 0.5°C and contour intervals of ±1 and 2°C are shown. Negative (cool) SST anomalies are shaded blue. Wind climatology period is 1968–96. SST climatology period is 1950–79. Both SST and wind data are from NCEP/NCAR Reanalysis and were obtained from http://www.esrl.noaa.gov.

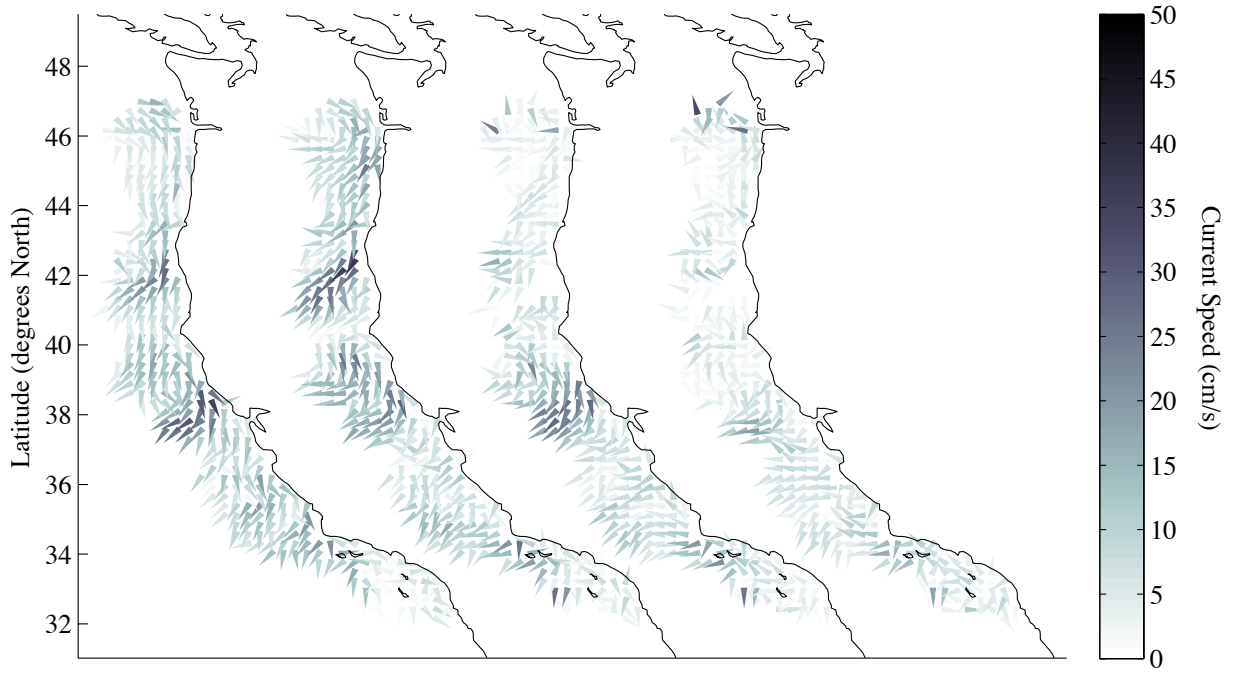

Figure 5. Mean maps of HF-radar surface currents observed quarterly throughout the CCS. From left to right, the panels present data for spring (March–May), summer (June–August), fall (September–November), and winter (December–February). Current speed is indicated by shading and direction given by orientation of arrow extending from observation location. For clarity, currents are displayed with spatial resolution of 30 km.

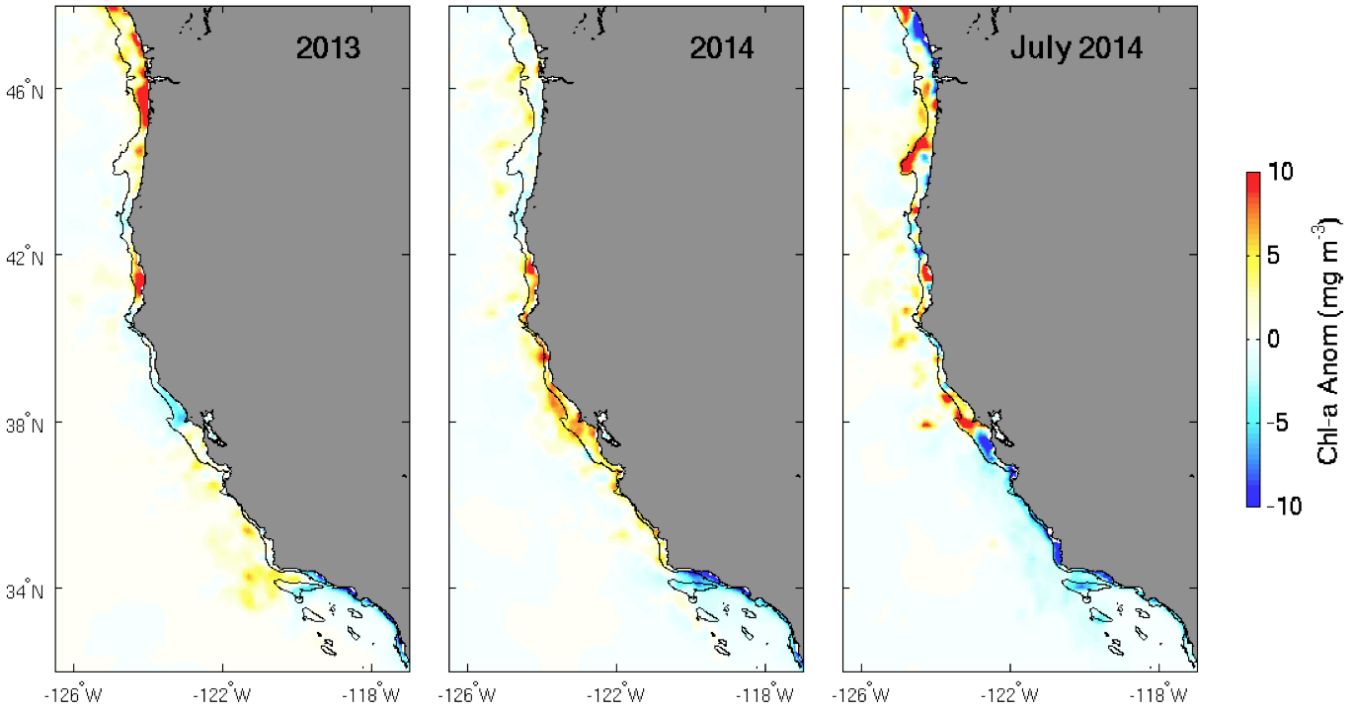

Figure 6. Chlorophyll *a* anomaly from Aqua MODIS, monthly composite (0.1 deg x 0.1 deg grid). Monthly climatology based on 2002–July 2014. 2013 March–May average anomaly (left panel), March–May 2014 average (center), and Jul 2014 only average (right panel).

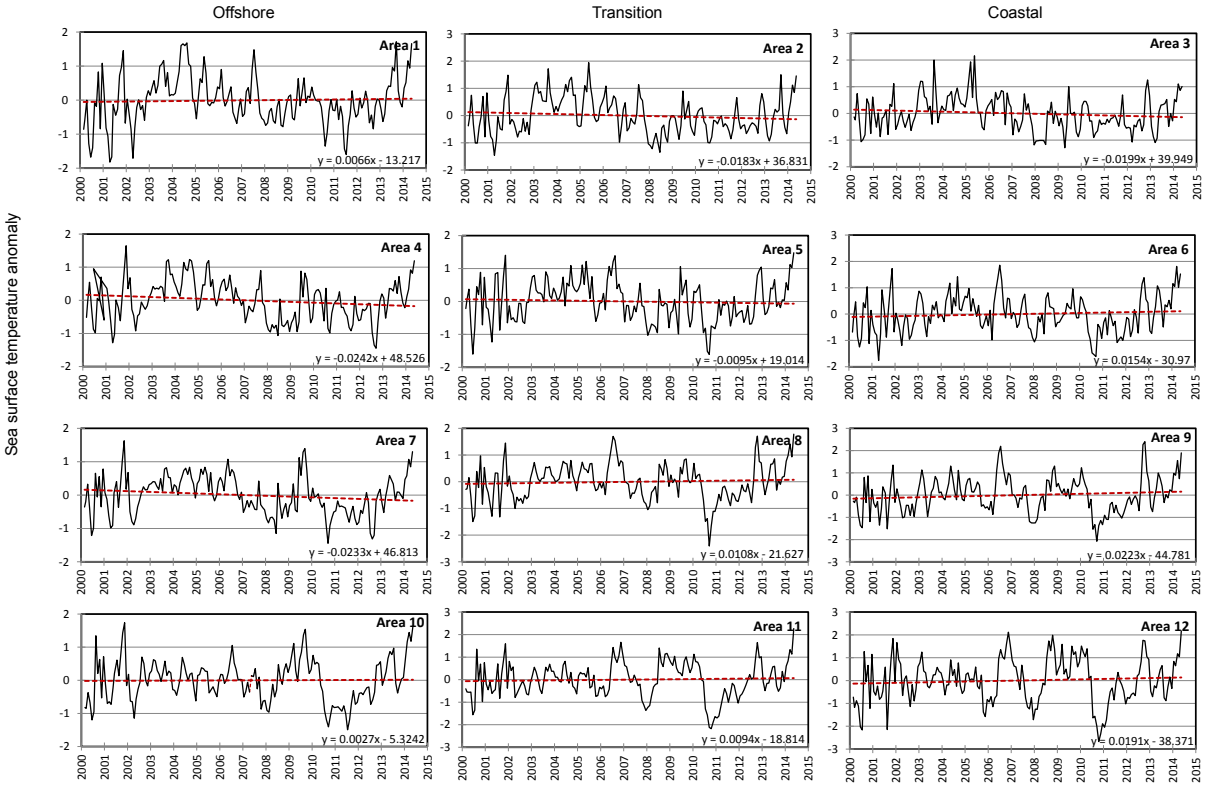

Figure 7. Time series of monthly mean SST anomaly (°C; black line) on the grid of 3 x 4 regions (fig. 1a red numbered grid). Monthly anomalies relative to the monthly means were calculated as the difference from the monthly mean. Red dashed line indicates long-term trend (mean and slope given in lower right hand corner of each panel).

ern California (southernmost location 46025: 33.749 N 119.053 W; supplement fig. S4). The cool SST in these months was associated with periods of strong southward winds driving upwelling (winds were typically at or very near 1 Standard Error level of the biharmonic annual climatic cycle; fig. S4). Warm SST were observed in June and August–September in locations north of San Francisco due to a reversal in the southward winds. By November 2013, winds were once again stronger southward than the climatological mean and SST in the north were low. In early 2014, SST were average to warmer than the climatological mean for all regions and all months except for the two most northern buoys (46050: 44.639 N 124.534 W, and 46027: 41.850 N 124.381 W), which experienced low SST in January and February due to the slackening of the northward winds in this region.

HF Radar Surface Current Observations

During 2013–14, surface currents observed were predominantly southward through spring, summer, and fall, with weak northward flows during winter in the southern and northern parts of the domain (fig. 5). While anomalous southward flows were persistent off Oregon during fall in 2013 (Sep–Nov), an equally anomalous northward flow was observed during the fall just north of Point Conception. The strong offshore flows (>30 cm s^{-1}) that are typically associated with headlands are most marked immediately off Point Arena (37°–39°N), and unusually, persisted through the 2013–14 winter. Also, south of Cape Blanco (41°–43°N), the offshore jet that typically develops during the upwelling season was stronger and more persistent than in other years (Wells et al. 2013; Bjorkstedt et al. 2012). Further south in the winter, a broad offshore flow was observed between Point Conception and Monterey Bay (34°–37°N), associated with convergence between southward flows to the north and northward flows to the south.

Satellite-Derived Surface Chlorophyll *a* and Temperature

Springtime 2013 anomalies (based on a monthly climatology measured by the Aqua MODIS satellite from 2002–May 2014) of chlorophyll *a* (March–May average) were high for most of the nearshore region, except for northern California (fig. 6). In contrast to 2013, the chlorophyll *a* anomalies during springtime 2014 were high for central California, but low in southern California and Oregon/Washington coast (fig. 6). By July 2014, this pattern had changed, with anomalously high values found in small patches from San Francisco Bay to Vancouver, with some low regions in between. The entire

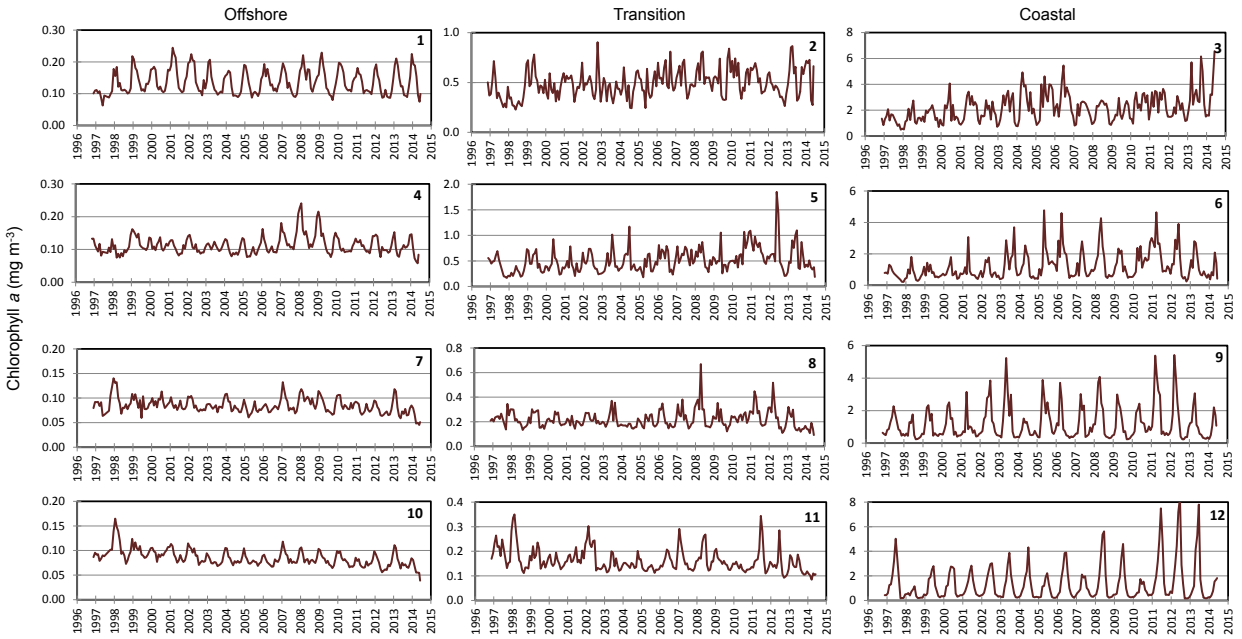

Figure 8. Time series of the monthly mean chlorophyll *a* merged from multiple satellite sensors (OCTS, SeaWiFS, MERIS, MODISA) on the grid of 3 x 4 regions (fig. 1a red grid).

southern portion of the nearshore region had anomalously low chlorophyll *a* levels (fig. 6).

Previous analysis of satellite-detected time series of surface chlorophyll *a* concentration (chlorophyll *a*, mg m^{-3}) in the California Current region from late 1996 to the end of 2011(Kahru et al. 2012) showed a statistically significant increasing trend of chlorophyll *a* in the coastal upwelling region of central California and significant decreasing trends of chlorophyll *a* in the central North Pacific gyre and off southern Baja California.

SST and satellite-detected surface chlorophyll *a* concentration (mg m^{-3}) was estimated from multiple ocean color sensors (OCTS, SeaWiFS, MERIS, MODIS-*a*qua) using empirical algorithms tuned to in situ measurements from the California Current (primarily CalCOFI and CCE-LTER; Kahru et al. 2012)[1]. Monthly anomalies relative to the monthly means were calculated as the ratio to the monthly mean for chlorophyll *a* or as the difference from the monthly mean for SST. The ratio anomaly was expressed as percentage anomaly with 100*(Anomaly – 1).

Warming was evident from the beginning of 2014 with SST anomalies up to +2°C at the beginning of June 2014 (fig. 7). SST anomalies were the weakest (+1°C) in the coastal region of central California (area 3, fig. 1 left panel). The approximately 18-year time series of surface chlorophyll *a* (fig. 8) shows spatially different trends. Correlated with the recent warming, chlorophyll *a* anomalies (fig. 9) turned negative approximately from the middle of 2013 in all areas except the coastal upwelling region of central California where they stayed positive. As a result, in the beginning of June of 2014, eleven regions had negative chlorophyll *a* anomalies and only one had a positive chlorophyll *a* anomaly.

REGIONAL ECOSYSTEM INDICATORS

Northern California Current: Oregon (Newport Hydrographic Line[1])

The winter of Dec 2012–Mar 2013 was quite mild with no large southwesterly storms, resulting in bottom waters on the midshelf that were colder and saltier than normal (saltiest and second coldest since 1997; not shown) at the baseline station (NH-5) off Oregon (45°N). These conditions continued during the spring (April–June) of 2013 when the second coldest temperature and third highest salinity values were observed since 1997 (fig. 10). The other "cold and salty" years were 2007 and 2008.

The day of spring transition in 2013 (based on the Cumulative Upwelling Index–CUI, fig. 3 45°N panel) was on 7 April, which was six days earlier than average (40-year climatology). Despite the near-average date of transition, upwelling continued to be weak through most

[1]After the end of data transmission from MERIS in April 2012, estimates of chlorophyll *a* are based solely on MODIS-*a*qua (MODISA) data. SST data were merged from MODISA and MODIS-Terra sensors from 2000 to end of May, 2014. Time series of monthly mean chlorophyll *a* were created on a grid of 3 by 4 areas (fig. 1, red grid) from offshore (~ distance from coast 300-1000 km) through transition zone (100–300 km from coast) to coastal zone (0–100 km from coast), and from north to south as central California (areas 1–3), southern California (areas 4–6), northern Baja California (areas 7–9) and southern Baja California (areas 9–12), following Kahru and Mitchell (2001) and Lynn and Simpson (1987).

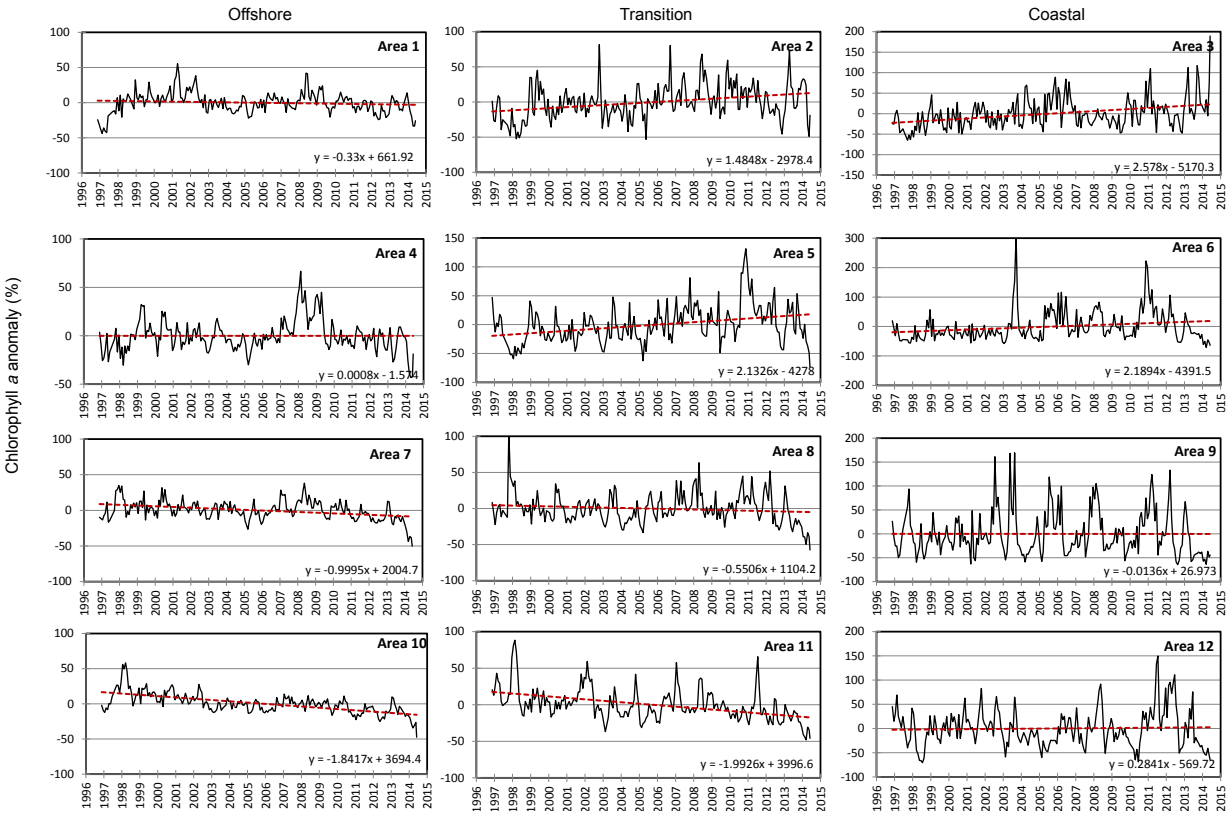

Figure 9. Time series of monthly chlorophyll *a* anomaly (%) on the grid of 3 x 4 regions (fig. 1a red numbered grid). Monthly anomalies relative to the monthly means were calculated as the ratio to the monthly mean. The ratio anomaly was expressed as percentage anomaly with 100*(Anomaly – 1). Red dashed line indicates long-term trend (mean and slope given in lower right hand corner of each panel).

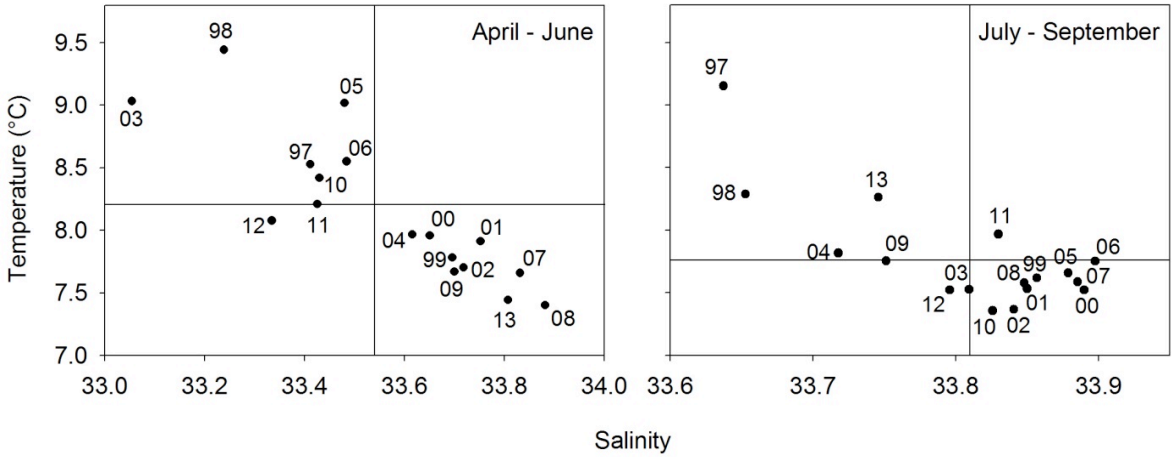

Figure 10. Seasonal mean temperature and salinity at 50 m depth at station NH-5 (Latitude: 44.6517 N Longitude: 124.1770 W) along the Newport Hydrographic Line for spring (left panel) and summer (right panel). Note changes in scale on both temperature and salinity axes. Numbers next to points indicate year of observations.

of May and June 2013, including a two-week period in mid-June of northeastward winds which resulted in warmer than average temperatures in July (fig. 11). Although the total upwelling from May–Sept was nearly the same as the 16-year average, most of the upwelling occurred during July through mid-August. Upwelling effectively ended in mid-September, three weeks earlier than climatology. The average temperature and salinity during the summer (July–Sept) were warm and fresh, respectively, compared to the typical values for this season, ranking the third and fourth warmest and freshest water observed during the upwelling season since 1997 (fig. 10). In fact, deep waters in summer 2013 were very similar to the 1998 El Niño event.

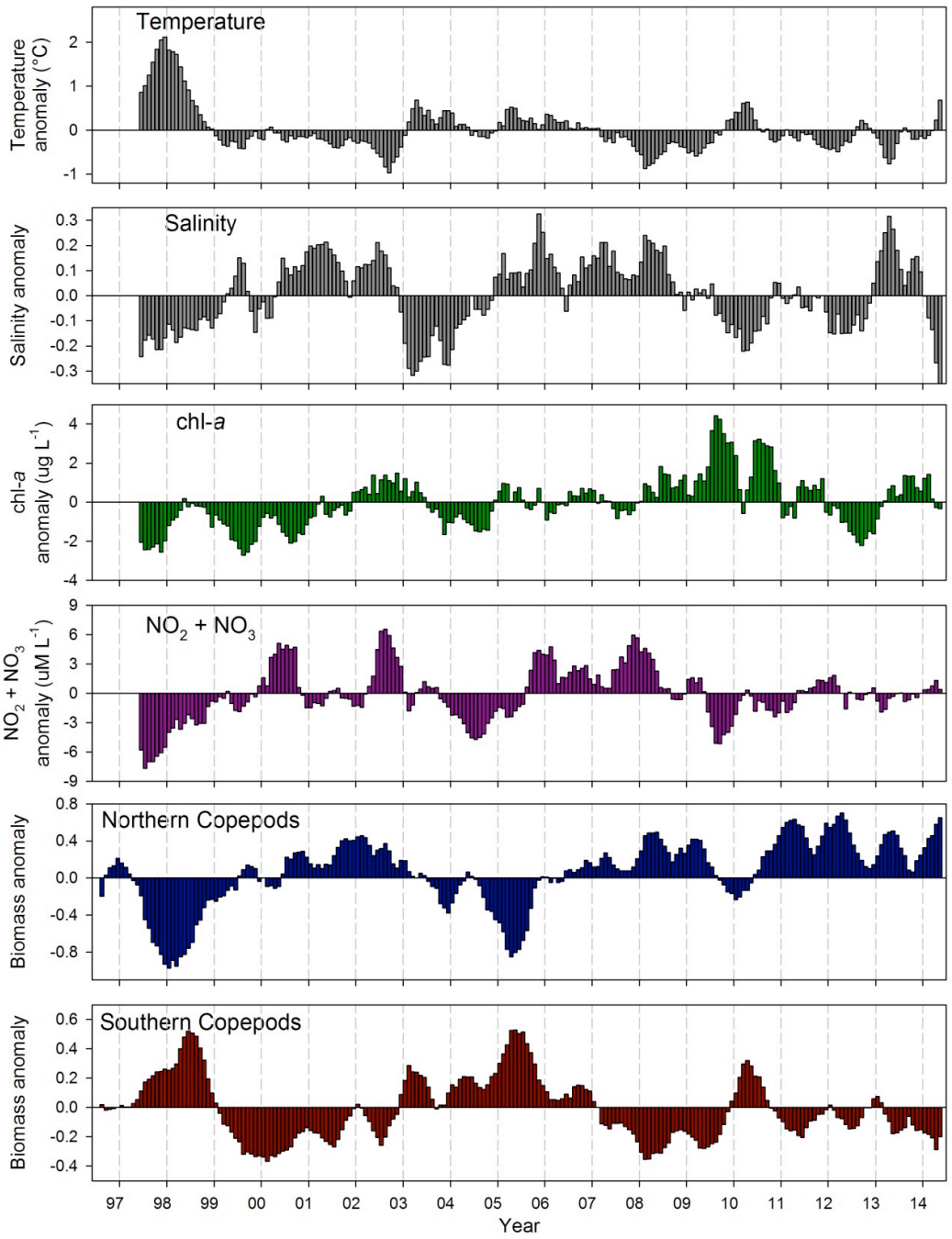

Figure 11. Time series plots of local physical and biological anomalies (monthly climatology removed) from 1997–present at NH-5 (Latitude: 44.6517 N Longitude: 124.1770 W) along the Newport Hydrographic Line. Temperature and salinity from 50 m, chlorophyll *a* and $NO_2 + NO_3$ from the surface and copepod biomass anomalies are integrated over the upper 60 m. All data were smoothed with a 7-month running mean to remove high frequency variability.

As for the copepods, during winter (Nov 2012–March 2013), the biomass of southern ("warm water") copepods was moderately high (fig. 11) compared to values from 2011–mid 2014, in correspondence with positive values of the Oceanic Niño Index during autumn 2012–winter 2013. In the spring (April–June) of 2013, the biomass of southern copepods was less than average and the biomass of northern ("cold water") copepods increased dramatically and remained high throughout the summer upwelling period (fig. 11). This increase in northern copepods was consistent with observations of high biomass of these boreal species since 2011 throughout the year, and generally followed strongly negative values of the PDO. However, the PDO during 2013 was only moderately negative yet northern copepod biomass was high.

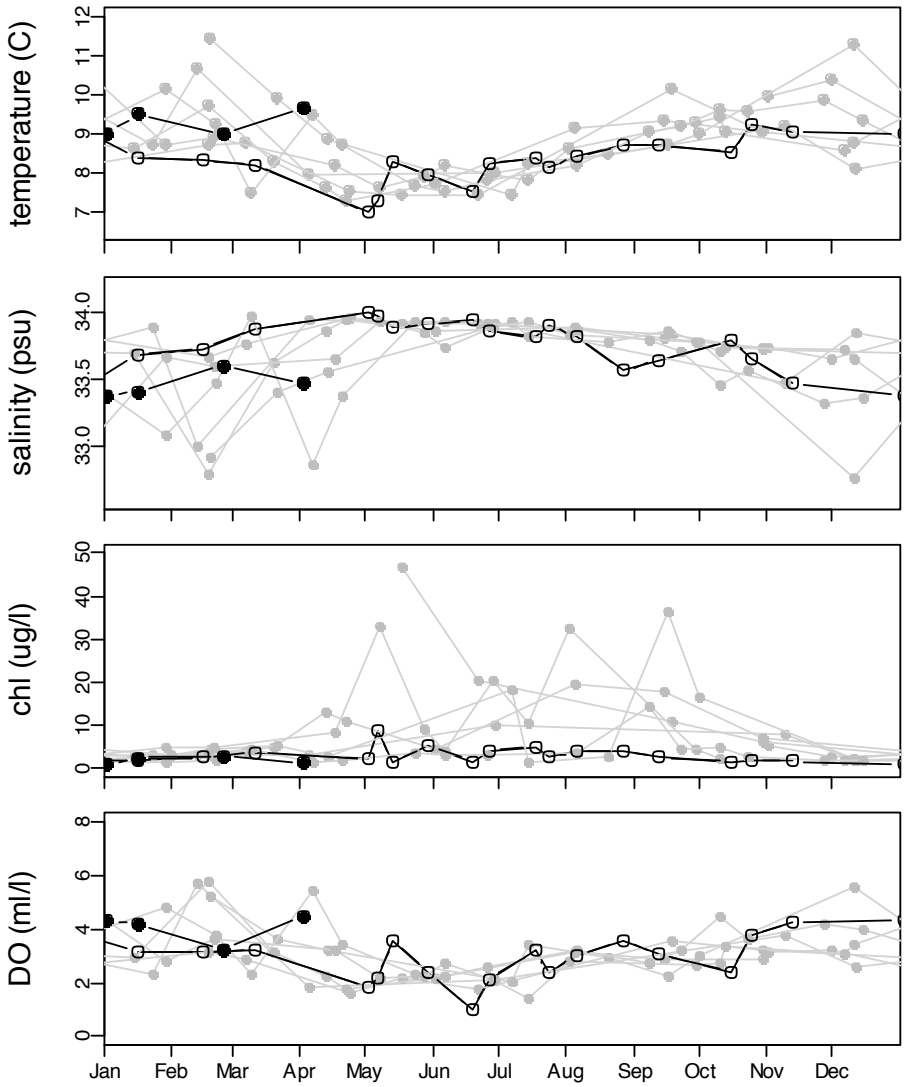

Figure 12. Hydrographic and ecosystem indicators at midshelf along the Trinidad Head Line (station TH02; 41°03.5' N, 124°16' W, 75m depth). Panels from top to bottom show near-bottom (60 m) temperature, near-bottom (60 m) salinity, mean chlorophyll *a* concentration over the upper 30 meters of the water column, and near bottom (60 m) dissolved oxygen concentrations. Grey symbols indicate historical observations (2006–12), unfilled circles indicate observations during 2013, and filled symbols indicate observations in 2014.

As we entered 2014, storms (which likely are reflected in the higher than average CUI values) were more frequent in winter compared to 2013, but similar to climatology. Average T-S values of deep shelf water at NH05 for the Jan–Mar 2014 period were near the long-term mean values (9.34°C and 32.8). Other aspects of ocean conditions in 2013 along with our forecasts of salmon returns can be seen at http://www.nwfsc.noaa.gov by selecting "Salmon Forecasts."[2]

Copepod data were based on samples collected with a 0.5 m diameter ring net of 202 μm mesh, hauled from near the bottom to the sea surface. A TSK flowmeter was used to estimate distance towed.

[2]Regular sampling of the Newport Hydrographic Line continued on a biweekly basis along the inner portions of the line (out to 25 nautical miles from shore). Details on sampling protocols are available in previous reports and at http://www.nwfsc.noaa.gov/research/divisions/fe/estuarine/oeip/ka-hydrography-zoo-ichthyoplankton.cfm.

Trinidad Head Line, Northern California

Temperature and salinity near the seafloor at midshelf were generally consistent with strong upwelling throughout much of the spring and early summer in 2013, and especially with consistent, strong southward winds that persisted throughout much of April and into June 2013 (fig. 12). Despite this strong upwelling, chlorophyll *a* concentrations remained relatively low over the shelf, possibly due to offshore advection or intense grazing. Dissolved oxygen reached the lowest levels observed in the 9-year time series in mid-June.

Observations of low dissolved oxygen (DO) over

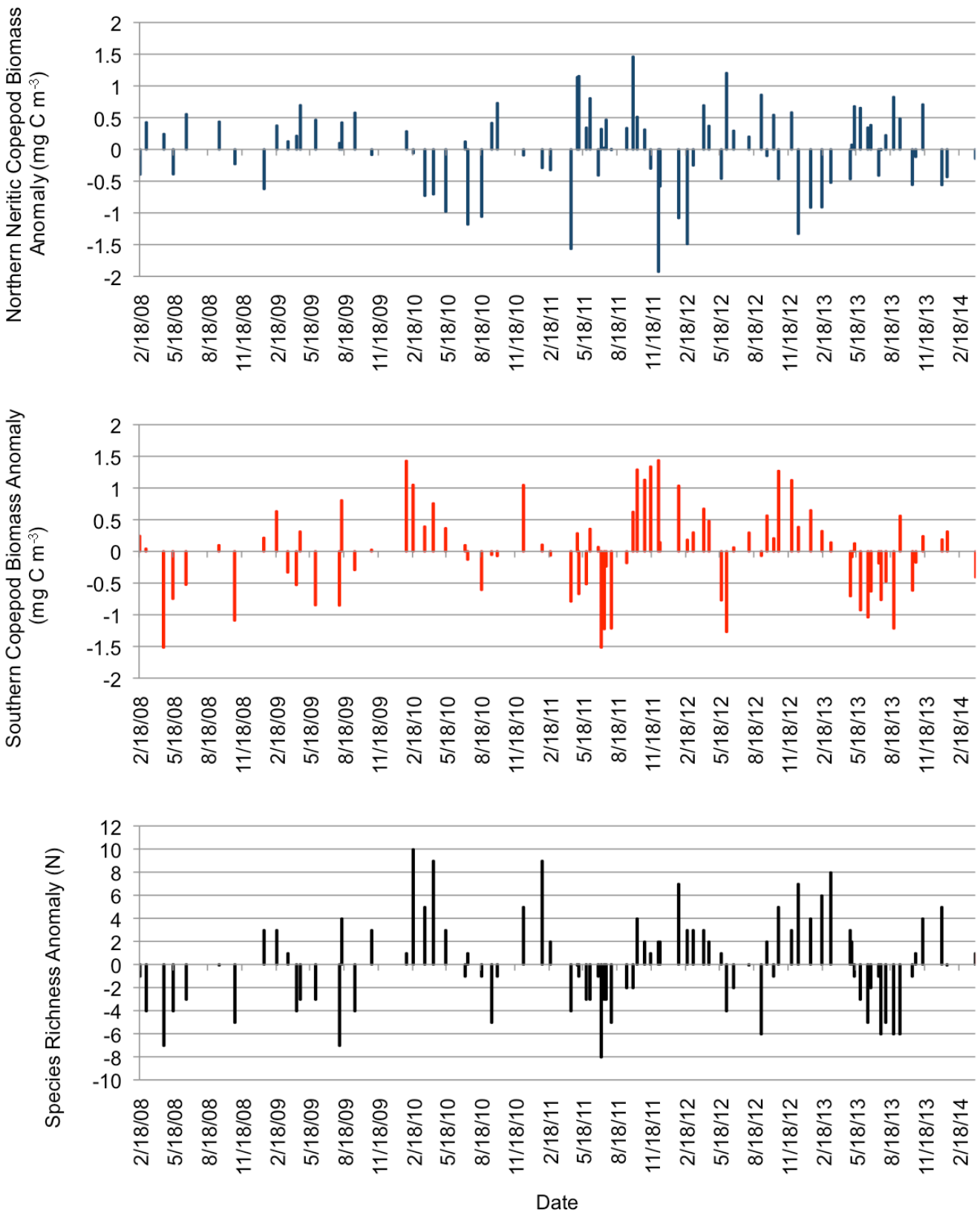

Figure 13. Anomalies (from the 2008–14 mean) in biomass and species richness of the copepod assemblage at midshelf on the Trinidad Head Line (station TH02; 41°03.5' N, 124°16' W, 75m depth). Upper panel: biomass anomaly of dominant northern neritic copepods (dominated by *Pseudocalanus mimus*, *Calanus marshallae*, and *Acartia longiremis*). Middle panel: biomass anomaly of southern copepods (neritic and oceanic taxa combined; dominated by *Acartia tonsa*, *Acartia danae*, *Calanus pacificus*, *Ctenocalanus vanus*, *Paracalanus parvus*, *Clausocalanus* spp., and *Calocalanus* spp.). Lower panel: species richness anomaly (N species).

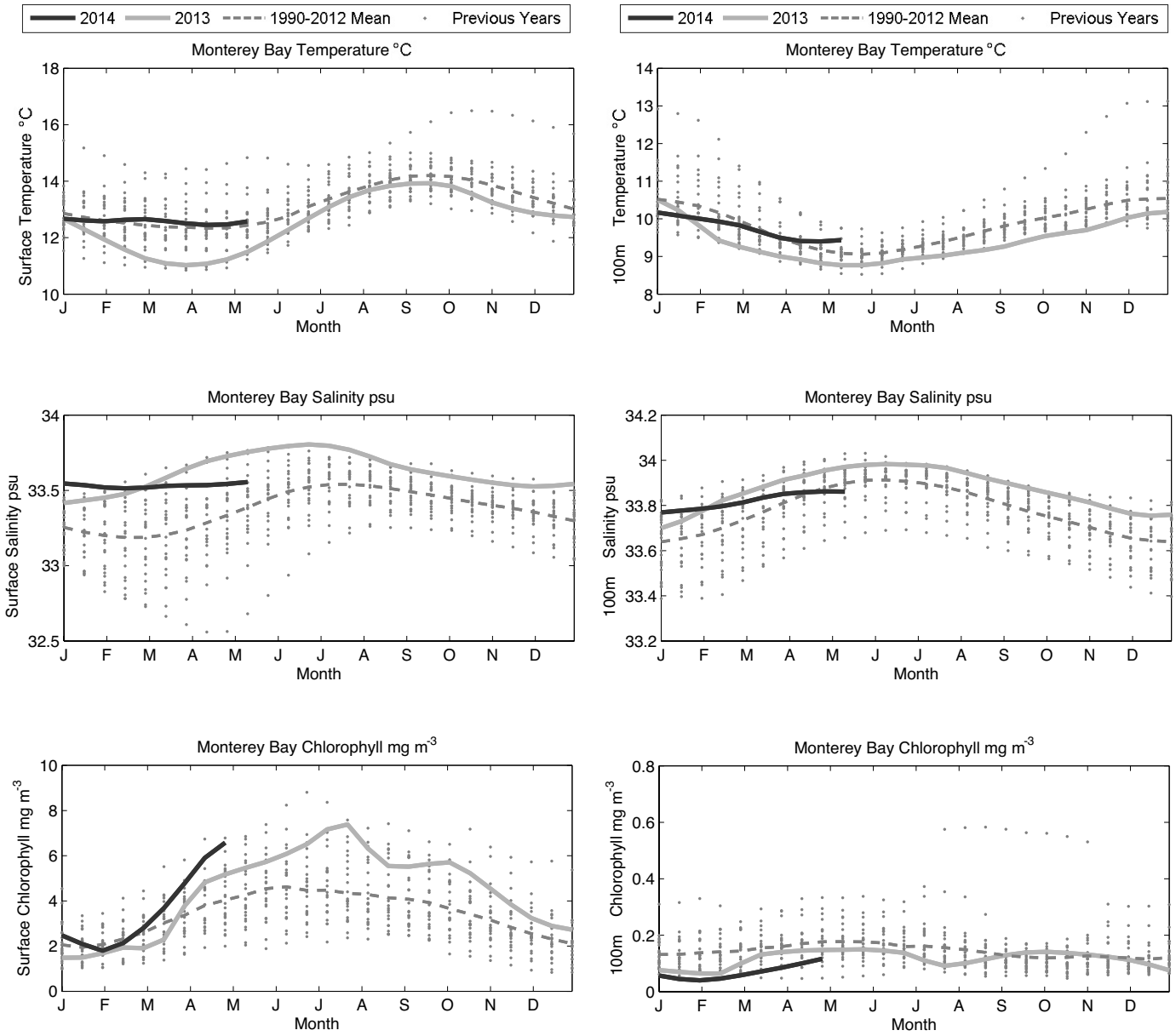

Figure 14. Temperature (top panels), salinity (middle panels) and chlorophyll *a* concentration (bottom panels) at the surface (left hand column) and at 100 m (right hand column) observed at the M1 mooring in Monterey Bay, CA.

the shelf in mid-June coincided with low DO/low pH detected at Trinidad Wharf (Frank Shaughnessy, pers. comm.; CeNCOOS data) during the intense upwelling in late May and early June. This event appears to have triggered an extensive stranding of krill (mostly *Thysanoessa spinifera*) in mid-June along beaches in northern California and southern Oregon following an unusual reversal to strong northward winds (see http://caseagrantnews.org/2013/07/01/sea-grant-studying-krill-die-off).

In contrast to early 2013, conditions in early 2014 have been consistent with very mild southward winds and greatly reduced storm activity along the north coast. More recently, southward winds have been consistently intense throughout May and into early June, and have triggered a substantial phytoplankton bloom over the shelf (data not shown).

During the spring and summer of 2013, the copepod assemblage at station TH02 showed a shift to northern neritic species, a clear decline of southern species, and concurrent decline in species richness than had been observed in 2012 (fig. 13). Although biomass of northern neritic species declined during the winter of 2014, the biomass of southern species did not reach levels observed during most past winters, again perhaps a consequence of limited northward winds and winter storms during the 2013–14 winter.

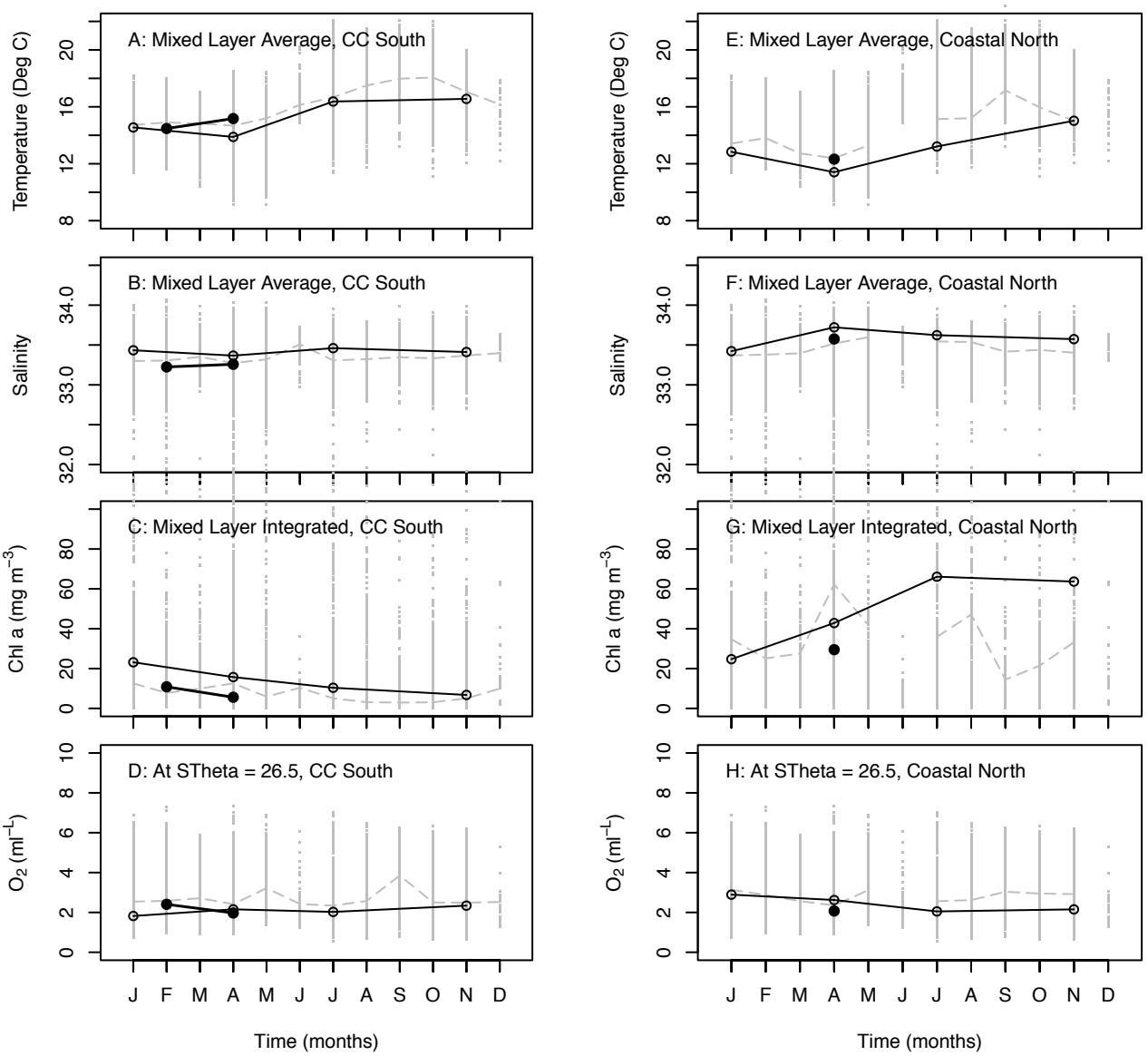

Figure 15. Average mixed-layer temperature (A+E), average mixed layer salinity (B+F), integrated mixed-layer chlorophyll *a* (C+G), and average O_2 concentration at the σ_θ 26.5 kg m^{-3} isopycnal, from the southern coastal region of the CalCOFI grid (CC South, left-hand column) and the north coastal region of the CalCOFI grid (Coastal north, right-hand column). Grey dots show averages for individual cruises from 1984–2012, dashed line shows climatological monthly average (1984–2012), line with open symbols shows 2013, and line with closed symbols is 2014. Note, the Feb 2014 cruise was cancelled partway through the cruise due to engine failure, thus there were no samples from the coastal north region.

MBARI, M1 Mooring, Central California

Temperatures in Monterey Bay were cooler than the 1990–2012 climatological mean during most of 2013 particularly at the surface during the spring (fig. 14), likely indicative of high upwelling (fig. 3). Salinities were also higher during 2013 than the climatological mean. Chlorophyll *a* was high at the surface during 2013, especially during the summer months. 2014 saw a shift to temperatures similar to the climatological mean through May, however salinity in the winter of 2013–14 remained high, with values decreasing towards the climatological mean by May. Chlorophyll *a* was relatively high at the surface in April and May 2014. Temperature and salinity followed a similar pattern at 100 m as at the surface, whereas chlorophyll *a* was lower than the mean for 2013-14 (fig. 14, right-hand panels).

CalCOFI Surveys, Southern California

Because the CalCOFI program samples an area large enough that it encompasses at least three somewhat distinct oceanographic zones, we have divided the area into three subregions for analysis, following Wells et al. (2013). The first subregion, "CC South," denotes the area landward of the main core of the California Current, south of Pt. Conception; essentially the Southern California Bight (CalCOFI lines 93–87, and stations 60–90). The

second region, "Coastal North," denotes the nearshore, upwelling-dominated region from Pt. Conception north to Pt. San Luis (lines 80–77, and stations <60). The third region, "Edge of North Pacific Gyre," is to the south and offshore, influenced by the subtropical gyre (defined by lines 90–93, and stations 100–120). Within each of these regions, we compared cruise-averaged mixed-layer temperature, salinity, integrated chlorophyll *a*, and oxygen at the σ_θ 26.5 kg m^{-3} isopycnal versus their respective climatological monthly means (based on 1984–2012).

In 2013, within CC South, average mixed-layer temperatures and salinity were similar to the climatological monthly means (figs. 15A, B, S6). Integrated chlorophyll *a* was higher (22, 18, and 15 mg m^{-2}) than the mean (14, 15, and 8 mg m^{-2}) during winter, spring, and summer cruises, respectively (fig. 15C, S9). In contrast, oxygen at the σ_θ 26.5 kg m^{-3} isopycnal was similar to the mean (fig. 15D). During spring 2014, temperatures were only slightly higher than average, whereas salinities and oxygen at the σ_θ 26.5 kg m^{-3} isopycnal were similar to the mean. Chlorophyll *a*, however, was lower (8 mg m^{-2}) than the spring mean (15 mg m^{-2}; fig. 15C).

In 2013, within the Coastal North subregion, temperatures were anomalously low (typically 1–2 degrees cooler) and salinities at the surface were high (typically 0.1 higher) as compared to the monthly means for the entire year (fig. 15E, S6), consistent with strong upwelling during this period (fig. 2). Oxygen was similar to the mean (fig. 15F, H), but chlorophyll *a* was much higher than the mean in summer and fall (>60 mg m^{-2} versus the mean of <40 mg m^{-2}; fig. 15G), again consistent with high upwelling during this period in this location. Profiles of chlorophyll *a* for this region showed a marked increase within the mixed layer compared to previous years and the long-term climatology (fig. S9c). The 2014 winter cruise was terminated before reaching region 2 (due to engine problems). 2014 spring temperature, salinity, and mid-depth oxygen were similar to the climatological mean, whereas chlorophyll *a* was anomalously low (28 mg m^{-2} compared to the mean of ~60 mg m^{-2}).

Averaging over the entire CalCOFI grid, mixed-layer temperatures were lower than the long-term mean (calculated from 1984–2014) by ~0.5°C in 2013, but above the mean by ~0.5°C in February and April 2014 (fig. S7a). Mixed-layer salinity, nitrate, and integrated primary production anomalies were also greater in 2013 compared to the long term mean (anomalies of 0.18 psu, 1 μg NO_3 L^{-1}, and 200 mg m^{-2} d^{-1}, respectively), but decreased during early 2014 (figs. S7, S8). The nitricline depth was deeper than the mean for all of 2013–14 (anomaly = –12 m), but shoaled somewhat from 2013 to 2014 (anomaly = –1 m; fig. S7d). Total zooplankton displacement volume was high in both 2013 and 2014 (average anomaly of +0.57 ln displacement volume; fig. S8).

REGIONAL PATTERNS IN FISH SPECIES

Northern California Current, Newport Line

Ichthyoplankton samples were collected from three stations representing coastal (<100 m in depth), shelf (100–1000 m), and offshore (>1000 m) regions along both the Newport Hydrographic (NH; 44.65°N, 124.35–125.12°W) and Columbia River (CR; 46.16°N, 124.22–125.18°W) lines off the coast of Oregon between June 15 and July 20 in 2007–13. In addition, ichthyoplankton samples were collected from five coastal-shelf stations along the NH line (44.65°N, 124.18–124.65°W) in winter (January–March) of 1998–2014. For the complete June–July and winter larval fish sampling methods, see Auth (2011) and Daly et al. (2013), respectively.

The ichthyoplankton community along the central-northern coast of Oregon in June–July 2013 was similar to the average community structures found in the same area and season during the previous six years both in terms of mean concentrations and relative concentrations of the dominant taxa, except compared to the anomalously high concentrations of northern anchovy found in 2011 (fig. 16). However, larval rockfish were found in the highest concentration in June–July 2013 of the seven-year time series, while larval northern anchovy were found in the lowest concentration since 2008.

The biomass of ichthyoplankton that were likely salmon prey in 2014 from winter collections along the NH line were low (total mean biomass = 2.7 mg C 10^{-3} m^{-3}) and ranked 16th in the 17-yr time-series (1998–2014), predicting low food conditions for juvenile salmon during the 2014 out-migration. The total biomass of all fish larvae was also low (mean = 12.5 mg C 10^{-3} m^{-3}, not just salmon prey; fig. 17). Also low was the proportion of the total larvae that have been identified as common salmon prey. Ocean conditions in late fall were predictive of winter larval fish biomass in January–March based upon the PDO, and 2013 October–December PDO would predict average winter larval biomass, but early 2014 NPGO values are negative suggesting poorer ocean conditions for juvenile salmon as they out-migrate. Additionally, the proportion of the total larvae considered important salmon prey was below average (ranked 13th out of 17 years at 21.6%; data range from a low of 7.4% in 2011, and a high of 95% in 2000). The community of winter ichthyoplankton in 2014 is grouped with 1998: an El Niño year. Current predictions suggest that 2014 has a very good chance of having El Niño ocean conditions, and we have found that El Niño ocean conditions can add uncertainty to our

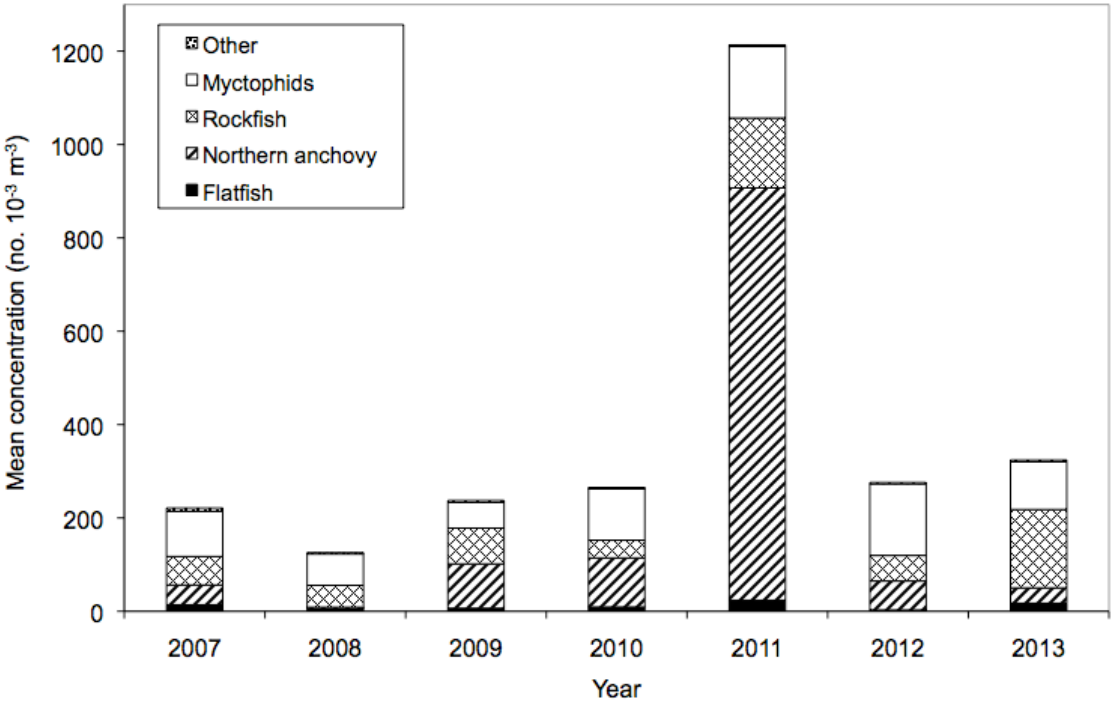

Figure 16. Mean concentrations (no. 10^{-3} m^{-3}) of the dominant larval fish taxa collected during June-July in 2007–13 along the Newport Hydrographic (NH; 44.65°N, 124.35–125.12°W) and Columbia River (CR; 46.16°N, 124.22–125.18°W) lines off the coast of Oregon.

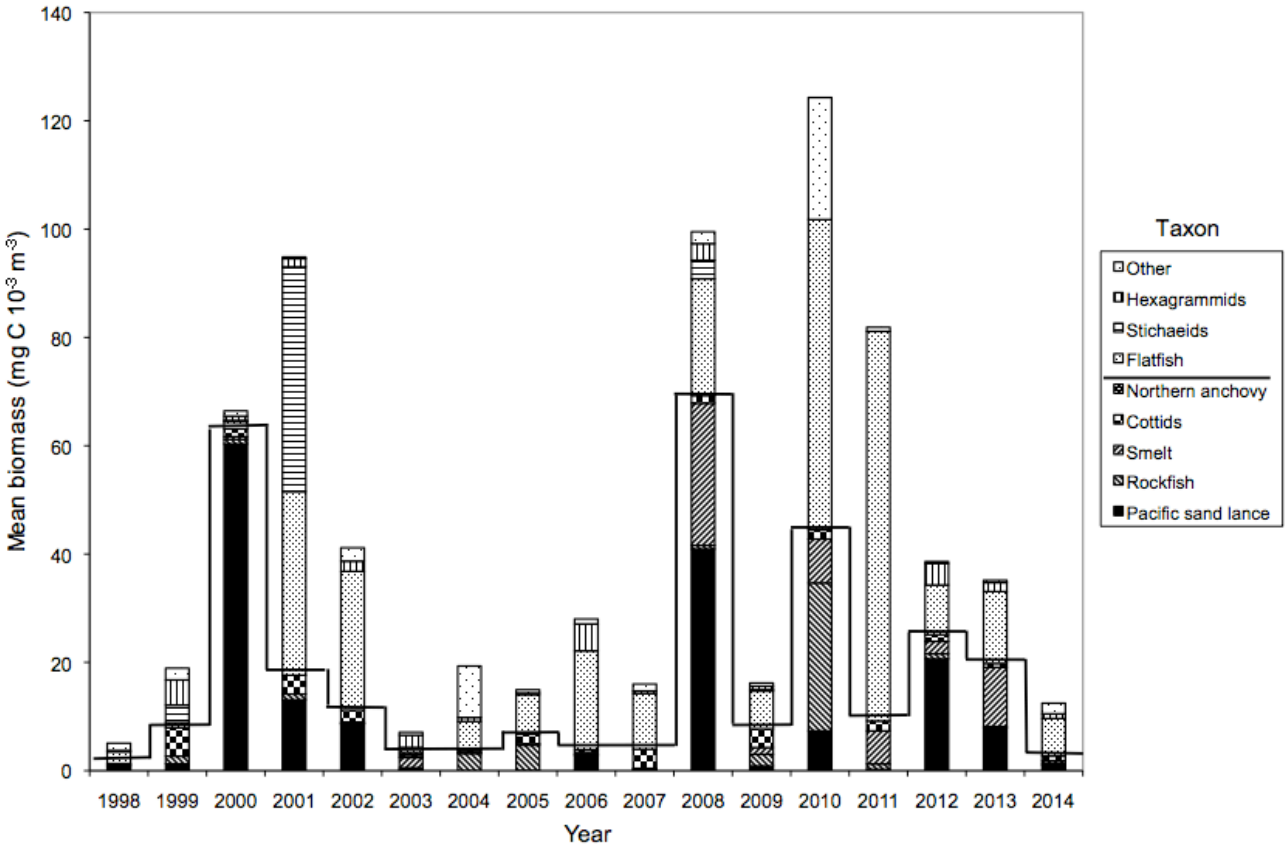

Figure 17. Annual mean biomass (mg C 10^{-3} m^{-3}) of the five important salmon prey taxa (below solid line) and four other dominant larval fish taxa (above solid line) collected during winter (January–March) in 1998–2014 along the Newport Hydrographic (NH) line off the coast of Oregon (44.65°N, 124.18–124.65°W). Figure expanded from one presented in Daly et al. (2013).

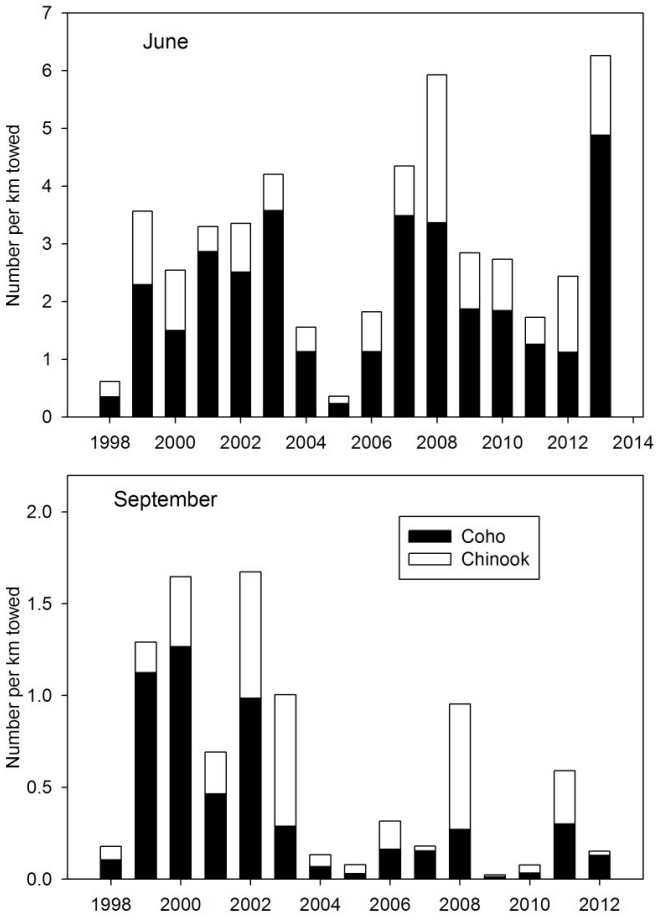

Figure 18. Catches of juvenile coho (black bars) and chinook (white bars) salmon off the coast of Oregon and Washington in June and September from 1998-present. Surveys were not conducted September 2013.

ability to accurately predict adult salmon returns. Overall, winter larval biomass and community structure would predict poor food conditions for juvenile salmon entering the ocean in 2014.

Northern California Current, Oregon and Washington Coast

Catches of juvenile coho salmon (*Oncorhynchus kisutch*) in pelagic rope trawl surveys off Oregon and Washington[19] were the highest in June 2013 since 1998 (fig. 18). Catches of juvenile (primarily sub-yearling) chinook salmon (*O. tshawytscha*) in June 2013 were about average. Due to funding constraints, there was no survey in September 2013.[3]

Pelagic fish catch data were collected by the NWFSC-NOAA Bonneville Power Administration survey surface trawls on standard stations along transects between La Push, WA and Newport, OR in June from 1999 to 2013. All tows were made during the day at predetermined locations along transects extending off the coast to the shelf break (Brodeur et al. 2005). We restricted the dataset to stations that were sampled consistently and >10 y over the sampling time period. Numbers of individuals were recorded for each species caught in each haul and were standardized by the horizontal distance sampled by the towed net as CPUE (#/km^2 towed). Yearly abundance data were obtained by averaging the standardized CPUE data across stations for each species sampled during the June survey. We restricted the species data to the top 15 abundant species captured in this dataset over the 14 years sampled years. We applied a Hellinger transformation (square root transformation of standardized row abundance values [Thompson et al. 2014]) to the species × year data set (15 species × 15 years), on which we ran a principal components analysis (PCA) ordination to describe the similarity of each year's community in species space (fig. 19). Additionally, we ran a two-way hierarchical cluster analysis on the yearly species community data with the Hellinger transformation. All community analyses were conducted in PC-ORD v.6.2 (McCune & Mefford 2011).

The resulting PCA ordination was 3 dimensional, explaining 94% of the total variance, with PCs 1, 2, and 3 (not shown) explaining 60.13%, 24.97%, 8.89% of the variability, respectively. Additionally, the loadings of the most abundant species in each PC were generated and are presented in Figure 20. Northern anchovy was strongly positively loaded onto PC 1 (0.74) whereas Pacific herring was strongly negatively loaded onto the same PC (0.65). Pacific sardine was strongly positively loaded onto PC 2. Salmonids (chinook, chum, and coho) were the species most loaded (negatively) onto PC 3 (0.58, 0.44, 053, respectively). 1999, 2001, and 2002 were anomalous years in terms of community structure during the surveyed time period relative to other years. A clear separation of these years from the rest is evident along PC 1 (fig. 19) and in the two-way cluster analysis (fig. 20). The separation of these years from the rest is due to the low abundance of anchovy and the relatively high abundance of herring during these years. There was also a dramatic shift in community composition between 1999 and 2000 and between 2000 and 2001. Some years showed remarkable similarities to other years. For example, based on the branch lengths of the cluster analysis, 2000 was very similar to 2005, 2007 and 2010, while 2003, 2004, 2009 and 2011 were very similar (fig. 21).

Ecosystem Indicators for the Central California Coast, May–June 2014

The Fisheries Ecology Division of the SWFSC has conducted an annual midwater trawl survey for juvenile rockfish (*Sebastes* spp.) and other pelagic micronekton along the central California coast in late spring (May–

[3] [19]Survey protocols are available at http://www.nwfsc.noaa.gov/research/divisions/fed/oeip/kb-juvenile-salmon-sampling.cfm.

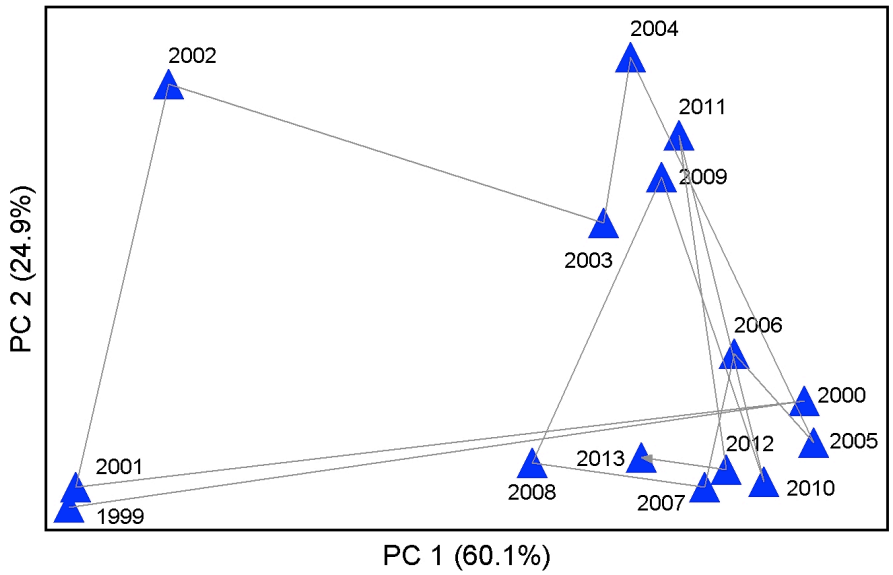

Figure 19. PCA of the yearly NCC pelagic fish community sampled between 1999 and 2013 in June off the Oregon and Washington coasts. The percentage variance explained by PCA1 and PCA2 are shown in parentheses on each axis.

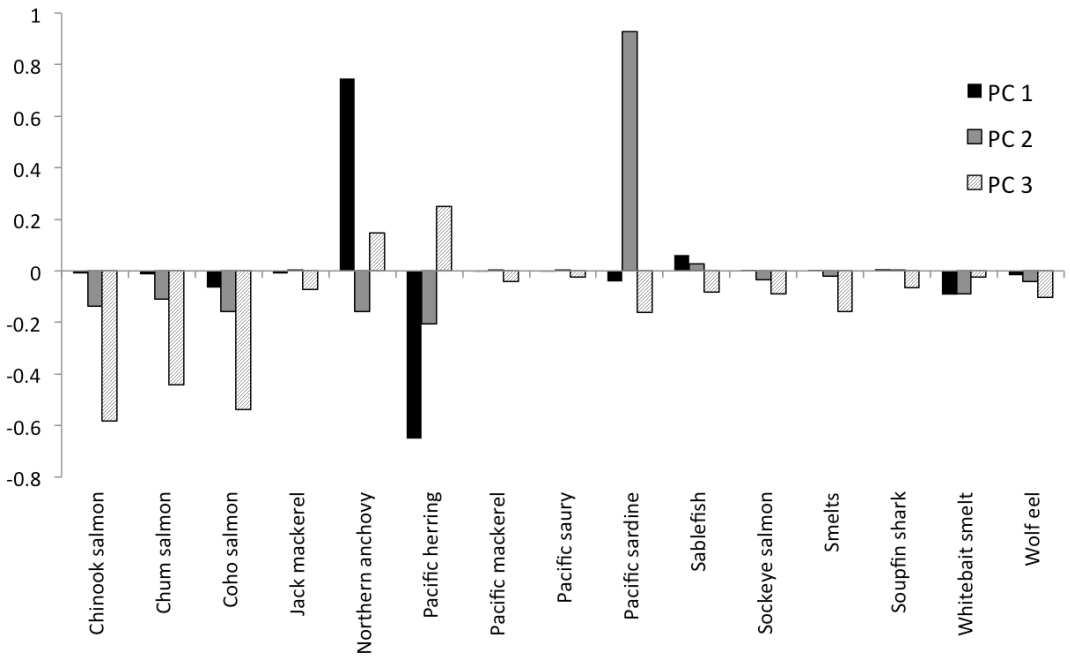

Figure 20. Top 15 abundant species loadings onto PCs 1, 2 and 3 of the 3-dimensional principal component analysis of the 15-year time series of surveyed pelagic fish in the northern California Current.

June) since 1983. Along with oceanographic information, the survey targets pelagic juvenile (young-of-the-year, YOY) rockfish and the micronekton forage assemblage (including other juvenile fishes, krill, coastal pelagic species, and mesopelagic species) for fisheries oceanography studies and stock assessments. The results here update a principal component analysis (PCA) of the pelagic micronekton community in the core area developed by Ralston et al. (2014). The data for the 2014 survey are preliminary. Trends from the southern (Southern California Bight) and northern (north of Point Reyes to Cape Mendocino) areas, which have been sampled only since 2004, were highly consistent with these "core area" trends for central California for most species. However, catches for juvenile groundfish and some other groups appeared to be below longer-term averages in much of the area north of Mendocino in 2014 (R. Brodeur, unpublished data). Differences in catch rates of YOY

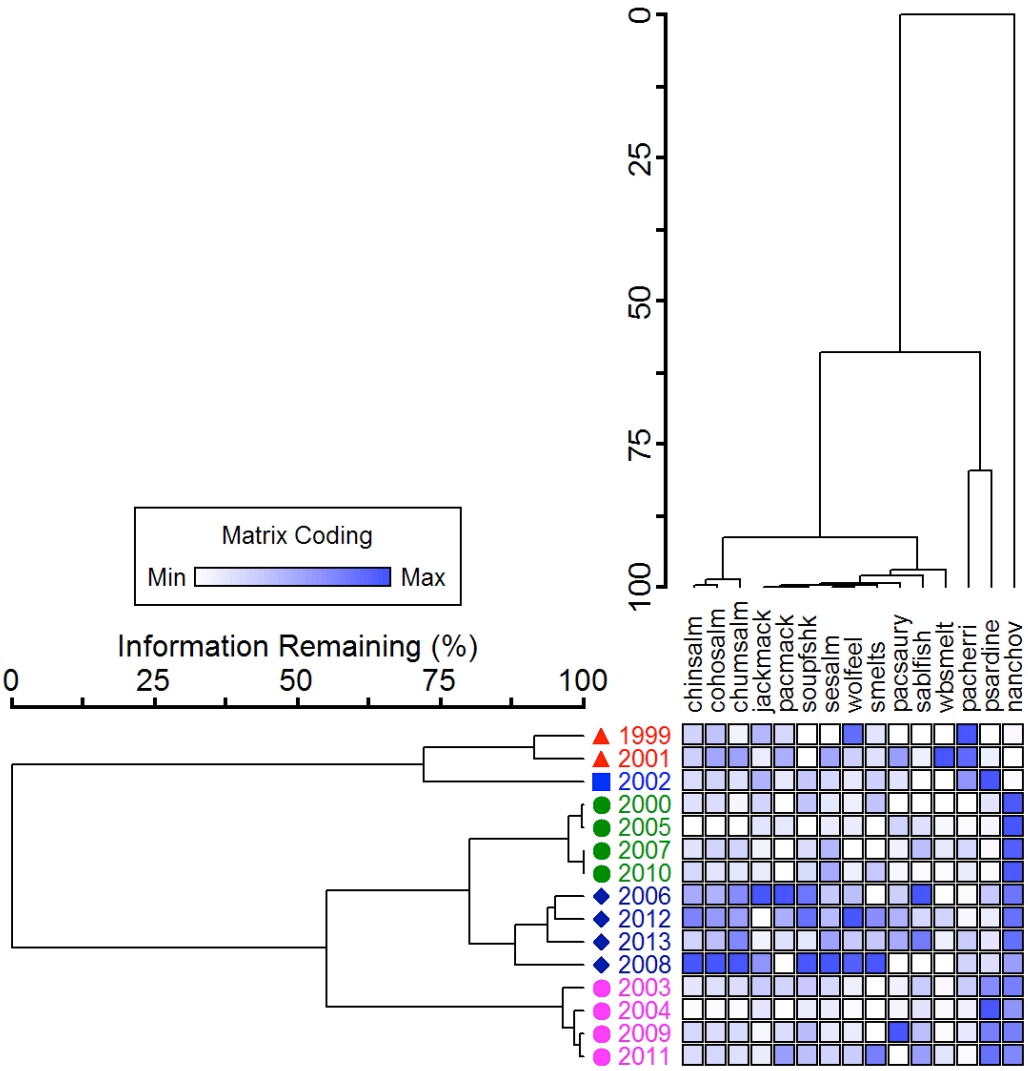

Figure 21. Two-way cluster dendrogram of yearly community composition. Matrix color-coding reflects the species average Hellinger transformed abundance in a given year. Yearly clusters defined at the 95% information remaining level.

rockfish have previously been described for these broad regions of the California Current (Ralston and Stewart 2013).

The standardized anomalies (based on 1990–2014 for central California and 2004–14 for the southern and northern regions, excluding 2012 for northern area) from the mean of the log (x+1) catch rates are shown by year for six key YOY groundfish and forage groups (fig. 22), including all YOY rockfish, market squid (*Doryteuthis opalescens*), krill (primarily *Euphausia pacifica* and *Thysanoessa spinifera*), YOY Pacific sanddab (*Citharichthys sordidus*), Pacific sardine (*Sardinops sagax*) and northern anchovy (*Engraulis mordax*). Notably, 2013 and 2014 had among the highest ever observed catches of juvenile rockfish, sanddab, and market squid in the core, southern and northern areas, following an unusually stable trend of high krill abundance and very low abundance of Pacific sardine and northern anchovy in preceding years. The longer time series for juvenile rockfish suggests that 1984 and 1985 were years of comparable high abundance for juvenile rockfish (Ralston et al. 2013). In both 2013 and 2014, these observations were consistent with high reported catches of YOY rockfish and other groundfish in power plant impingement surveys, scuba surveys, commercial and recreational fishermen, and from food habits studies of seabirds and other predators in this region.

An additional 14 species and groups were included in the analysis of the forage assemblage developed by Ralston et al. (2014), and are included in the PCA (fig. 23). The additional YOY groundfish groups include Pacific hake (*Merluccius productus*), speckled sanddab (*C. stigmaeus*), rex sole (*Glyptocephalus zachirus*), and lingcod (*Ophiodon elongates*). The remaining spe-

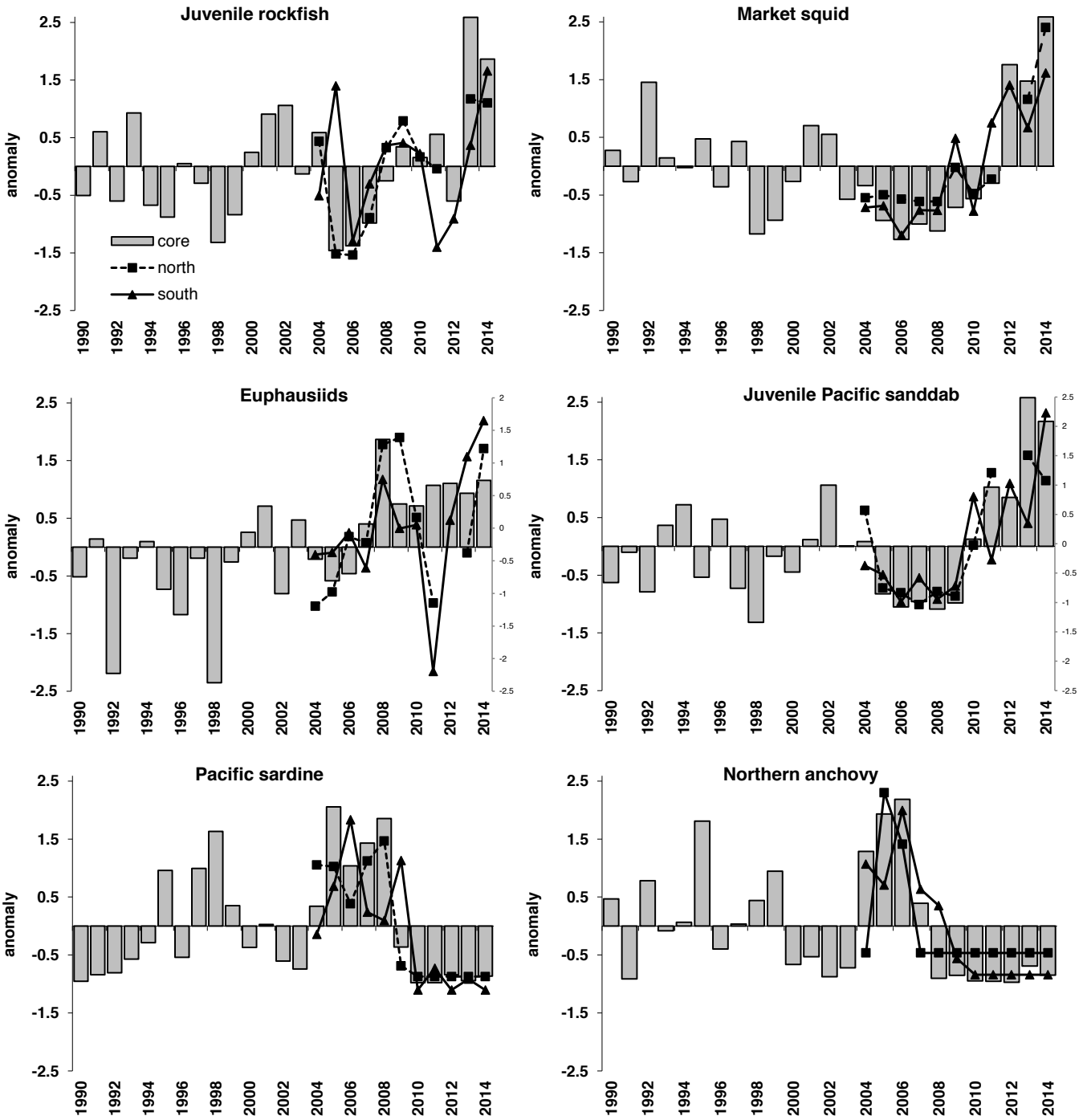

Figure 22. Long-term standardized anomalies of several of the most frequently encountered pelagic forage species from rockfish recruitment survey in the core (central California) region (1990–2014) and the southern and northern California survey areas (2004–14, excluding 2012 for the northern area).

cies and groups in the assemblage include adult Pacific hake, pelagic octopus, sergestid shrimp, gobies (family Gobiidae), plainfin midshipman (*Porichthys notatus*), and a variety of mesopelagic species. YOY groundfish, market squid, krill and several other taxa had strong positive loadings on PC 1 (which explained about 30% of the total variance, the first three PCs explained a total of 61% of the variance), with northern anchovy, Pacific sardine, and most mesopelagic species loading strongly negative on PC 1. This PC was not significantly related to basin-scale environmental indicators, such as the PDO, MEI, and the NPGO, but strongly related to both localized physical conditions (salinity, density and depth of the σ_θ 26.0 isopycnal) and indica-

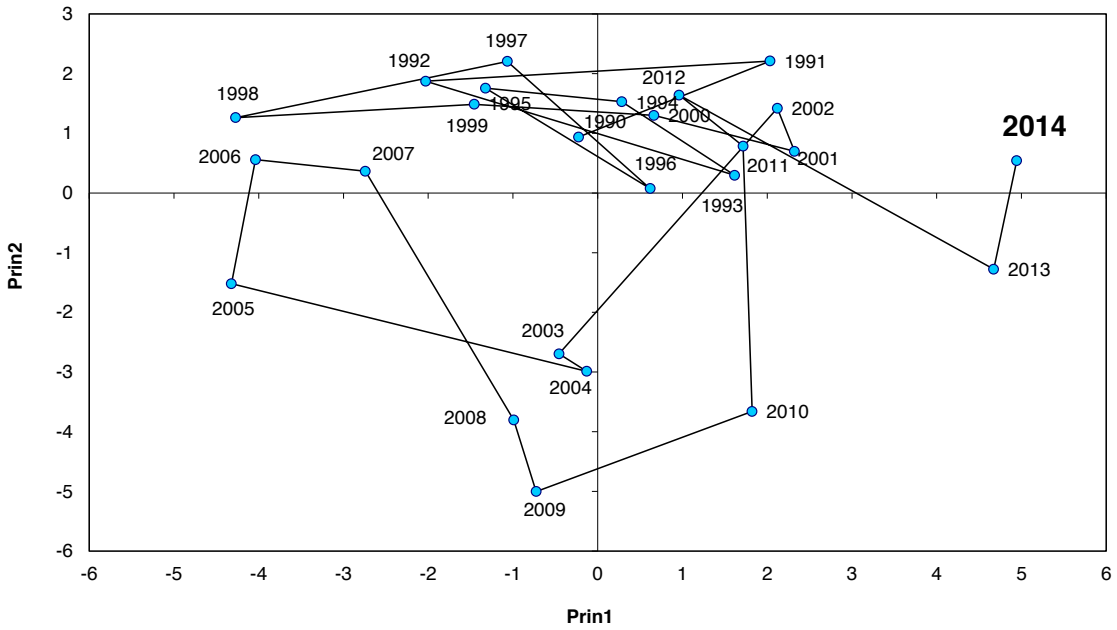

Figure 23. Principal component scores plotted in a phase graph for the twenty most frequently encountered species groups sampled in the central California core area in the 1990–2014 period.

tors of large-scale transport (AVISO sea surface height anomalies), such that the YOY rockfish, squid, and krill groups were more abundant during cool, high transport conditions. The second PC tended to load more strongly on the mesopelagic community, but relate poorly to environmental indicators, while PC 3 had strong loadings on a suite of taxa and was highly correlated to basin-scale climate indicators (see Ralston et al. 2014 for details).

The two leading PCs for the assemblage are shown in Figure 23, and the dramatic separation of 2013 and 2014, as being extremely orthogonal to the low productivity years of 1998, 2005, and 2006, is an indicator of the very high productivity of the cool-water, high transport assemblage in the last two years. Such shifts have important implications for higher trophic level species (such as seabirds, marine mammals, salmon, and adult groundfish) that forage primarily or exclusively on this assemblage. The observed dynamics of the YOY groundfish and high turnover invertebrates is thought to largely represents shifts in productivity associated with higher survival of early life-history stages for these species, while the trends observed for coastal pelagic and mesopelagic species (which load negatively on PC 1 and positively on PC 2) are thought to be more likely related to shifts in their distribution and consequent availability to the midwater trawl (e.g., Song et al. 2012; Wells et al. 2013). Although abundance of salps in the 2013–14 period did not reach the peak observed levels of 2012, the abundance of pyrosomes was the highest recorded in this survey (fig. 24).

Ecosystem Indicators for the Southern California, CalCOFI Region

The spring CalCOFI and Coastal Pelagic Species (CPS) surveys of 2014 yielded very few sardine eggs or larvae from either the continuous underway fish egg sampler (CUFES, fig. 25) or the vertical PairoVet net tows (see McClatchie 2014 and references therein for methods, survey domain, and descriptions of equipment). Spatial coverage by the two surveys was comparable to earlier years (fig. 26), but the only sardine ichthyoplankton encountered were in very low numbers and very nearshore in the Southern California Bight. 2014 is a low point in the time series since the sardine began to increase in the late 1980s (fig. 26; note the different scales for figs. 25 and 26). Only 17 adult sardine were captured by trawls during the 2014 spring CPS survey, and there were insufficient fish or eggs to permit the calculation of a reliable biomass estimate from either the daily egg production method (DEPM) or acoustics. We speculate that at such low abundance, the sardine distribution was very patchy, and sparse patches were not efficiently sampled by the survey design. The sardine fishing industry (Diane Plescher, California Wetfish Producers Association, personal communication) reported significant catches of sardine off central California early in the season, after which the fish disappeared. Although the survey took place from 28 March to 6 May, a large portion of the central coast was not surveyed until the latter half of April. It is unknown whether the fish spawned earlier than this, whether they began their seasonal northward migration early, or whether they were distributed fur-

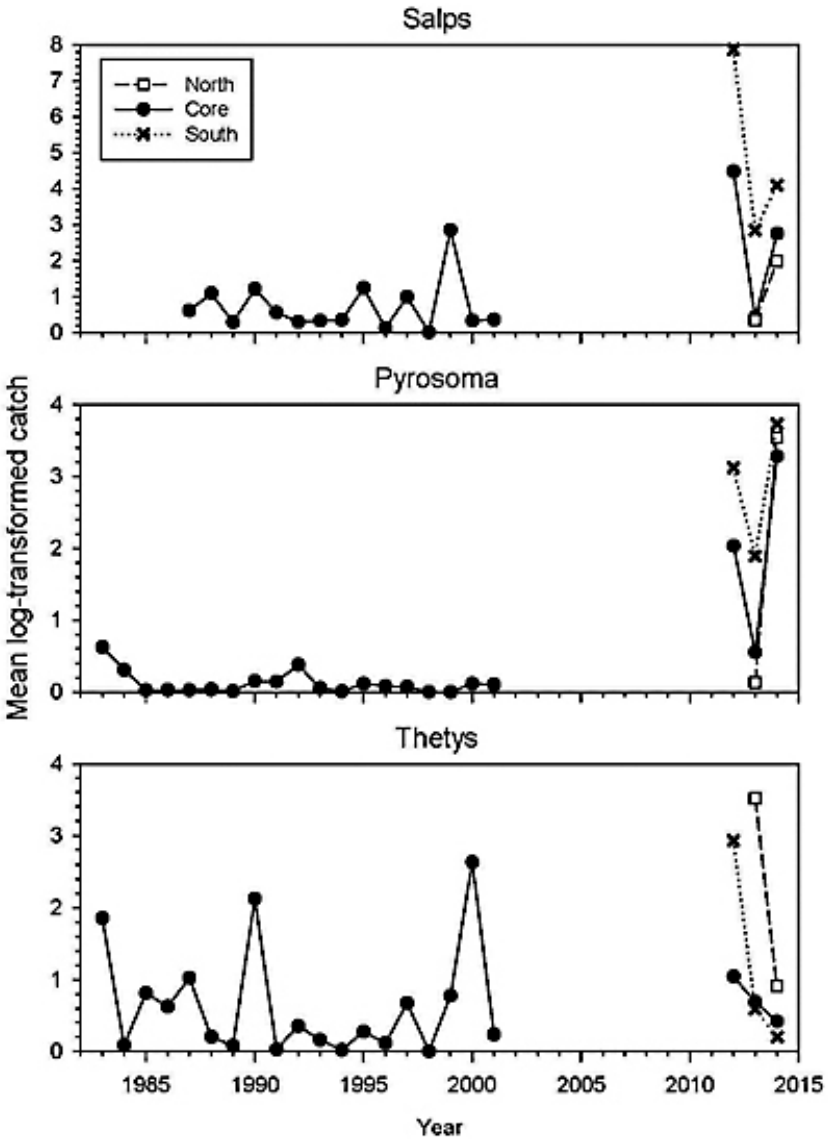

Figure 24. Geometric mean of catches per unit volume of gelatinous zooplankton from the rockfish recruitment survey.

ther offshore than the survey domain. Anchovy numbers also remained low and were distributed close to shore in the Southern California Bight (fig. 25). This was consistent with observations of low abundance of anchovy ichthyoplankton in recent years (Wells et al. 2013). Jack mackerel were the most abundant CPS ichthyoplankton in spring 2014 (fig. 25). Jack mackerel eggs were more abundant off southern California than off the central coast, and eggs were relatively close to shore in the southern region. In summary, the numbers of CPS ichthyoplankton were low in spring 2014, raising some unanswered questions regarding changes in distribution and timing of spawning. The very low sardine egg abundance and scarcity of sardine adults will make it difficult to accurately estimate population biomass for the sardine stock assessment.

REGIONAL PATTERNS IN BIRDS AND MARINE MAMMALS

Common Murres at Yaquina Head, Oregon

Median hatch date for common murres at Yaquina Head in 2013 was 4 July, similar to some previous years but a week later than we observed in 2012. Only 41% of the eggs laid hatched a chick (hatching success) and 24% of the eggs laid produced chicks that fledged (reproductive success; chicks ≥ 15 days were considered fledged). Reproductive success in 2013 was similar to 2011 and 2012, but less than half of the previous 4 years (2007–10, fig. 27) and the third lowest recorded for this colony. Only the reproductive success in 2010 and during the 1998 El Niño were slightly lower (Gladics et al. in review).

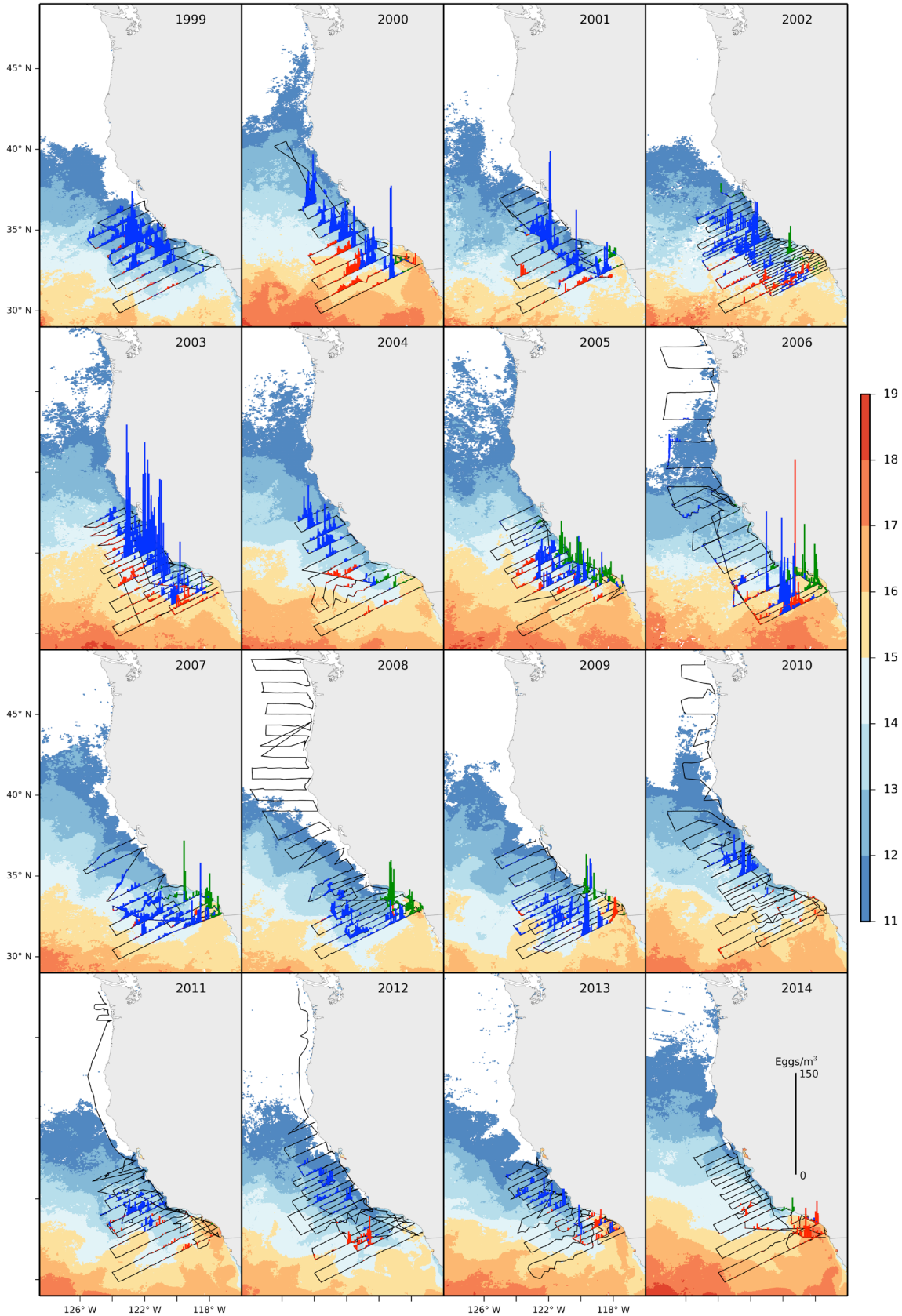

Figure 25: Density of eggs of sardine (blue), anchovy (green), and jack mackerel (red) collected with the continuous underway fish egg sampler (CUFES) overlaid on satellite sea surface temperatures (°C) derived from a monthly composite of April AVHRR Pathfinder imagery (1999–2008) and a blended SST product (2009–14). Ship track is shown by the black line. Colorbar indicates SST (°C).

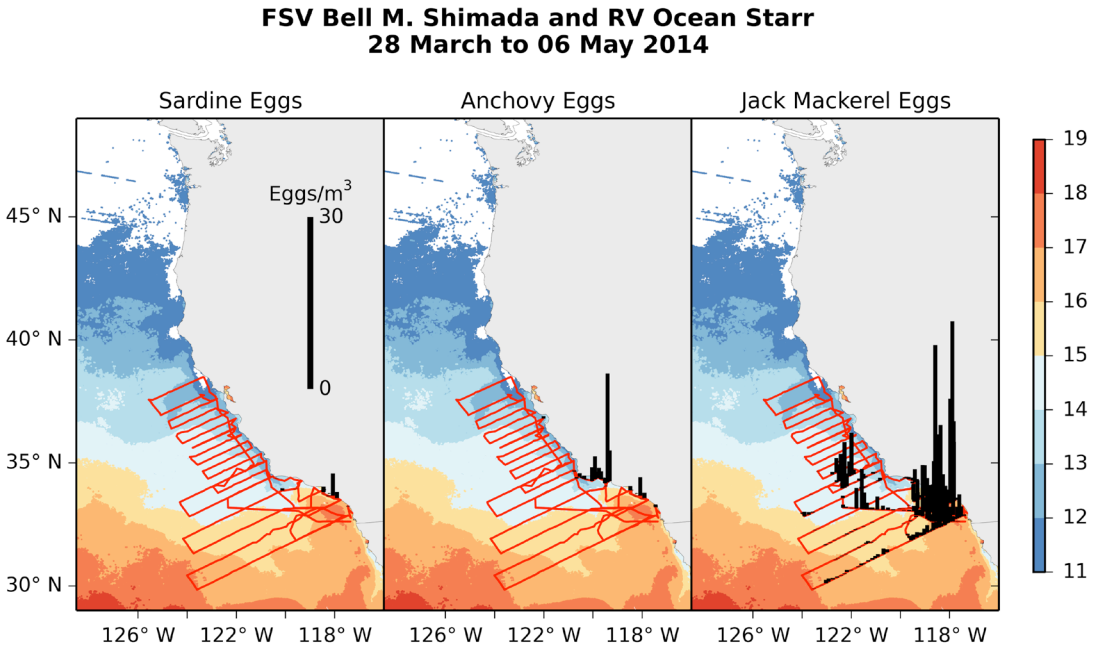

Figure 26: Density of eggs of sardine, anchovy, and jack mackerel collected with the continuous underway fish egg sampler (CUFES) during the spring 2014 CalCOFI and coastal pelagic fish cruises overlaid on satellite sea surface temperatures (°C).

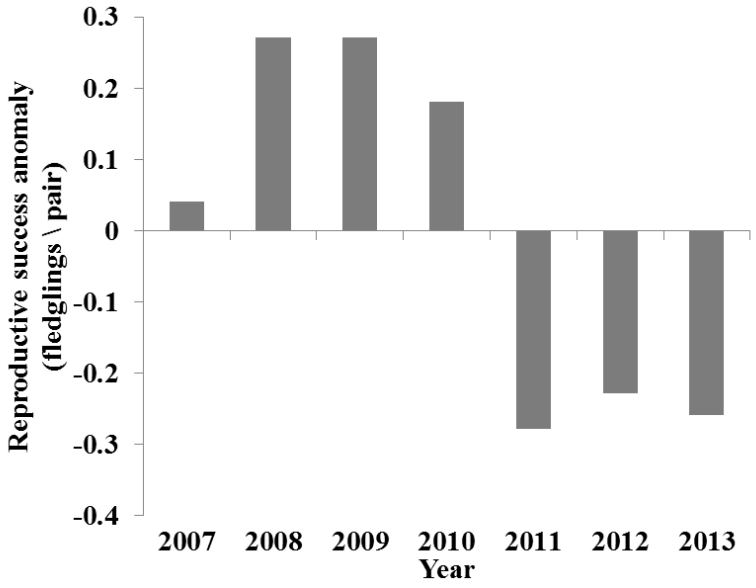

Figure 27. Anomalies of reproductive success for common murres nesting at Yaquina Head, Oregon, 2007–13.

Like the previous two seasons, much of the reproductive loss in 2013 was due to egg and chick predators. The total number of disturbances and the rate of murre egg and adult loss in 2013 were lower than the previous two years but higher than 2007–10. Disturbance rates first began to increase in 2010, and then greatly escalated in 2011, 2012, and 2013 (Horton 2014). The rate of adults killed per hour of observation was similar to those observed in both 2011 and 2012. Bald eagles (*Haliaeetus leucocephalus*) were again the dominant disturbance source (93%, 75 of 80 disturbances), unlike in 2012 when bald eagles caused only half of the disturbances (47%, 104 of 220 disturbances). Also unlike in 2012 when juvenile brown pelicans (*Pelecanus occidentalis*) resorted to eating fish regurgitated by murre chicks or eating murre chicks directly (Horton and Suryan 2012), there were no dramatic disturbances caused by pelicans in 2013, and pelicans were not observed landing on the colonies until the majority of murres had fledged. As of June 2014, we are seeing an early arrival of pelicans,

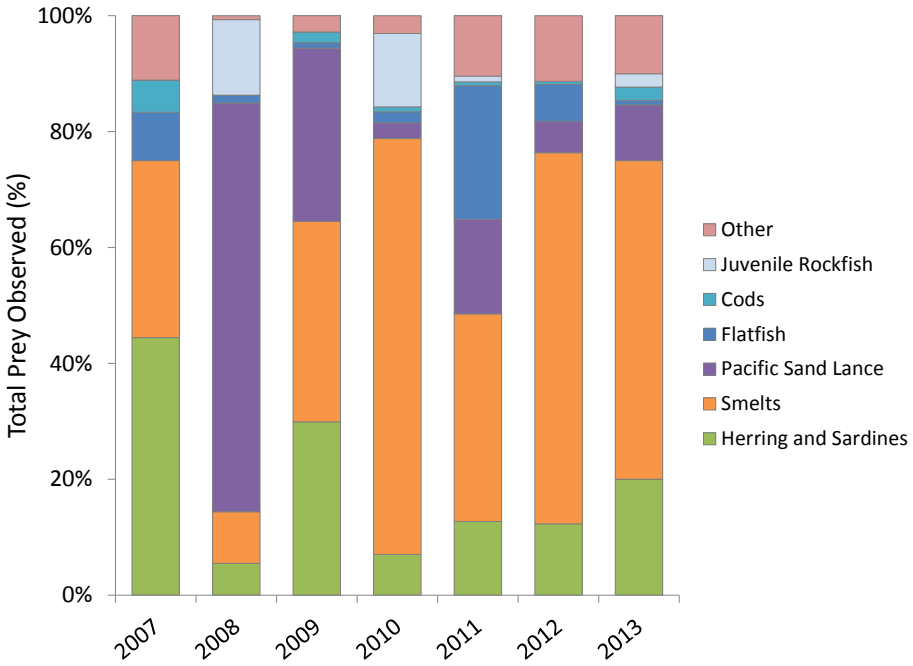

Figure 28. Prey fed to common murres chicks (% occurrence) at Yaquina Head Oregon, 2007–13.

likely resulting from their failed breeding attempts in the southern CCS and early northward departure from the breeding grounds.

Murre diets at Yaquina Head have varied annually. Forage fish species consumed in 2013 included primarily smelt (Osmeridae) and secondarily Pacific herring or sardine (Clupeidae) and Pacific sand lance (*Ammodytes hexapterus*) (fig. 28). A notable difference in diets among the past six years was the dominance of sand lance (associated with cooler waters) in 2008, and the dominance of smelt in 2010, and the increased consumption of flatfishes in 2011. Results show 2013 as intermediate with less smelt than 2010, but more than other years, somewhat similar to 2012. Clupeids (primarily Pacific herring, *Clupea pallasii*), which are generally associated with warmer water and positive PDO (Gladics et al. in review), increased slightly, but overall has remained low in the diets since 2009.

Summary of Common Murre Reproductive Success, Phenology, and Diet at Castle Rock National Wildlife Refuge: 2007–13

Castle Rock National Wildlife Refuge (hereafter Castle Rock) is a large common murre breeding colony in northern California near Crescent City, just south of Point St. George. The reproductive success, nesting phenology, and chick diet have been studied since 2007 using a remotely controlled camera monitoring system that was installed at the colony in 2006. The percentage of nests that successfully fledged young in 2013 was based on 75 nests that were monitored every other day. During 2013, 79% of nests fledged young, which was 6% greater than the long-term average for this colony (fig. 29). Nesting commenced on 22 April, 1 day later than the year with the earliest nest initiation (2009) and 22 days earlier than year with the latest nest initiation (2012; fig. 30). Diet observations occurred for an average of 80 hours each year while common murre chicks were present. In 2013, a total of 13 prey types were identified and prey composition was generally similar to other years, with smelt (Osmeridae) being the predominant prey fed to chicks and juvenile rockfish being the second most common prey fed to chicks (fig. 31).

Breeding Success of Seabirds at Southeast Farallon Island

The 2013 seabird breeding season at Southeast Farallon Island, California, was a very productive year for all species with Brandt's cormorants (*Phalacrocorax penicillatus*), pelagic cormorants (*Phalacrocorax peligacus*), and Cassin's auklets (*Ptychoramphus aleuticus*) exhibiting exceptionally high breeding success. Piscivorous common murres (*Uria aalge*), rhinoceros auklets (*Cerorhinca monocerata*), and pigeon guillemots (*Cepphus columba*), also had productive years with higher productivity than last season and also above the long-term mean (fig. 32). Western gulls (*Larus occidentalis*) rebounded from four straight years of very poor breeding success and fledged chicks at a rate equivalent to the long-term mean. Cassin's auklets, though declining slightly from 2012, con-

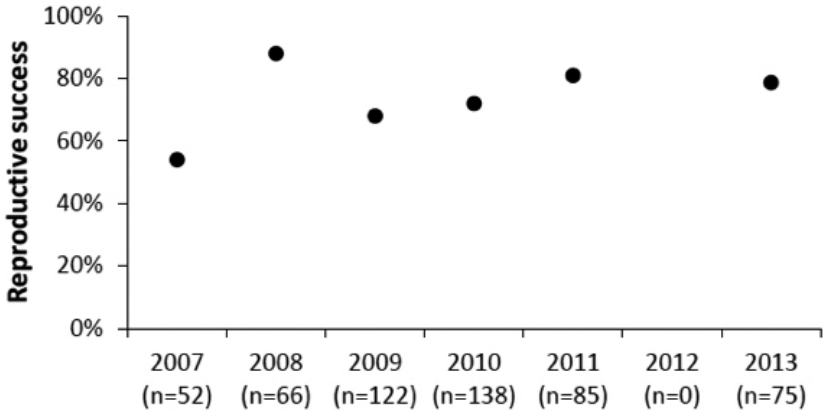

Figure 29. Percentage of common murre (*Uria aalge*) nests that successfully fledged young between 2007 and 2013 at Castle Rock National Wildlife Refuge, Del Norte County, California. The sample size (n) represents the total number of nests observed per year. This figure does not include the success of second clutches. Reproductive success could not be determined in 2012 due to early failure of the video monitoring system.

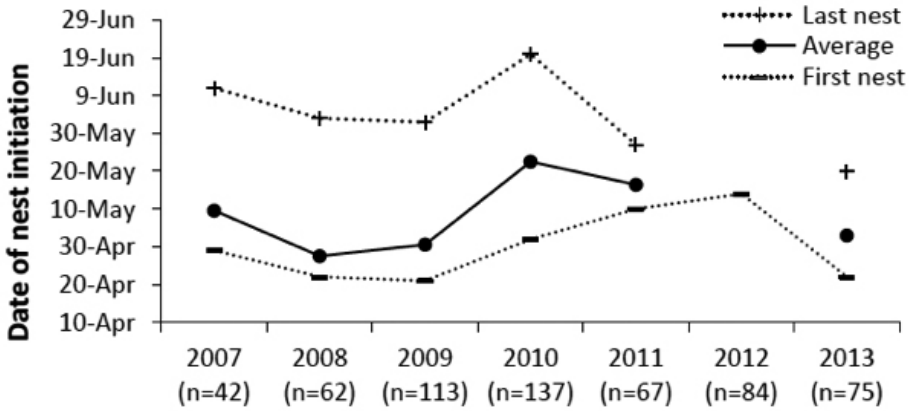

Figure 30. First, average, and last dates for nests initiated by common murres between 2007 and 2013 at Castle Rock National Wildlife Refuge, Del Norte County, CA. The date of nest initiation was the defined as the day that an egg was laid at a nest-site. The sample size (n) represents the total number of nests observed each year where nest initiation dates were accurate to ±3.5 days. The average and last date of nest initiation could not be determined in 2012 due to early failure of the video monitoring system.

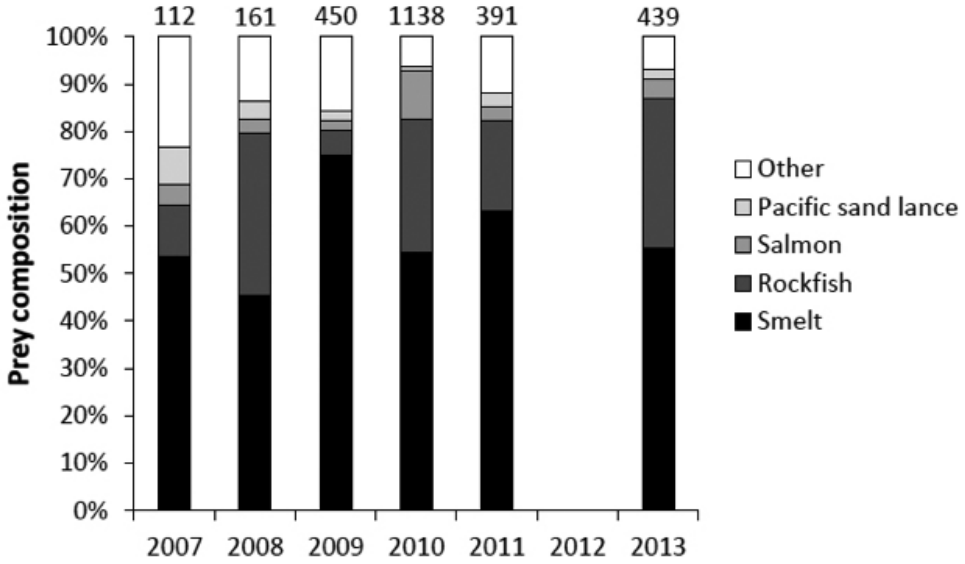

Figure 31. Composition of prey delivered to chicks by common murre between 2007 and 2013 at Castle Rock National Wildlife Refuge, Del Norte County, California. Numbers above each bar indicate the total number of prey identified each year. Prey composition could not be determined in 2012 due to early failure of the video monitoring system

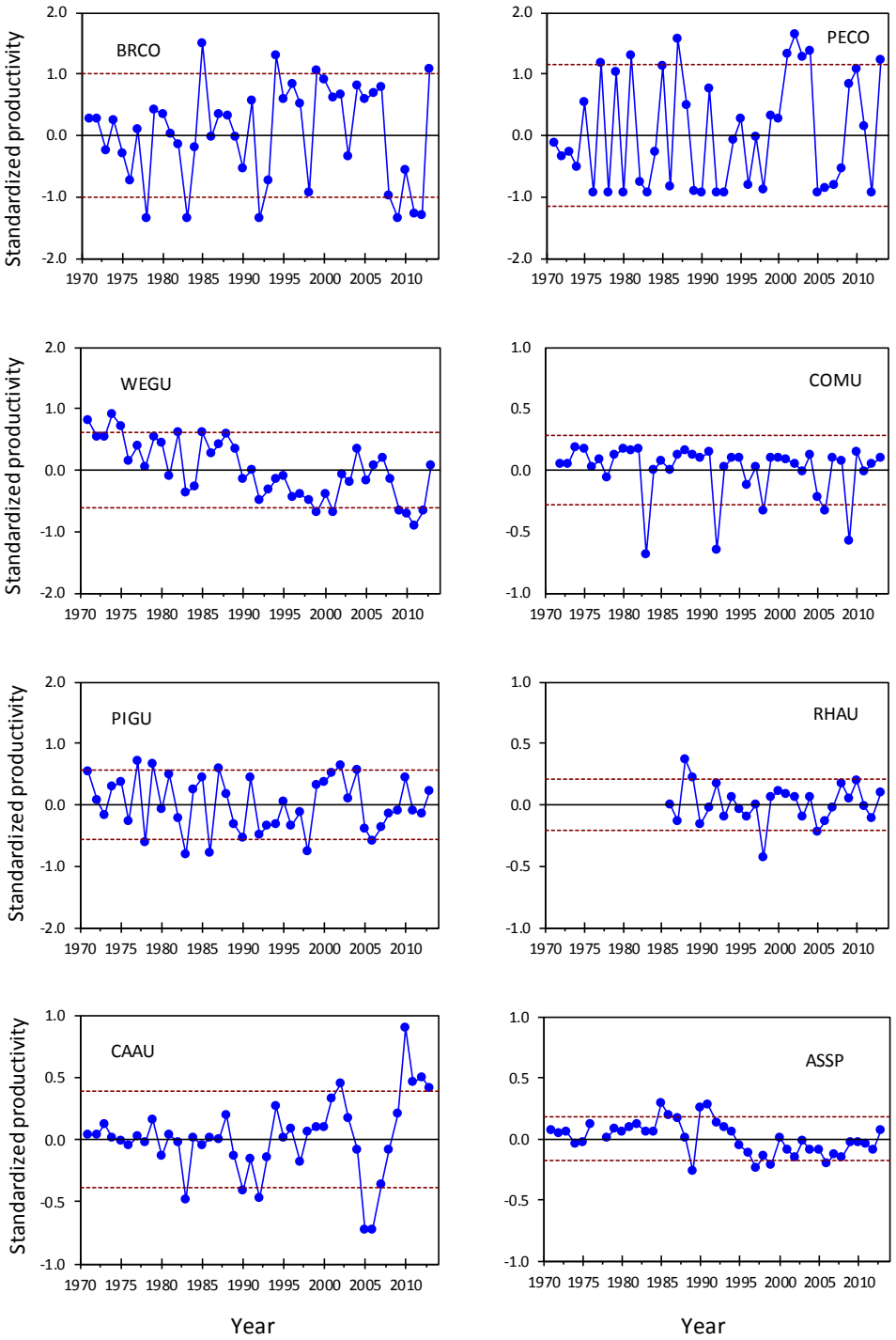

Figure 32. Standardized productivity anomalies (annual productivity–long term mean) for 8 species of seabirds on SEFI, 1971–2013. The dashed lines represent the 80% confidence interval for the long-term mean.

tinued to exhibit exceptionally high productivity with the 2013 productivity value within the top five years since studies began in 1972. This marks the fourth consecutive year of exceptional reproductive performance for Cassin's auklets. Auklet success was once again driven by abundant prey resources (primarily euphausiids) and a high rate of successful double brooding. Reproductive success of common murres was also higher than 2012 as well as being above the long-term mean for this species. Murres seemed to thrive once again on a high abundance of juvenile rockfish in the chick diet. Feeding rates were high, chicks grew quickly and fledging success was high. It appears that cormorants benefited from heavy foraging on juvenile rockfish as well.

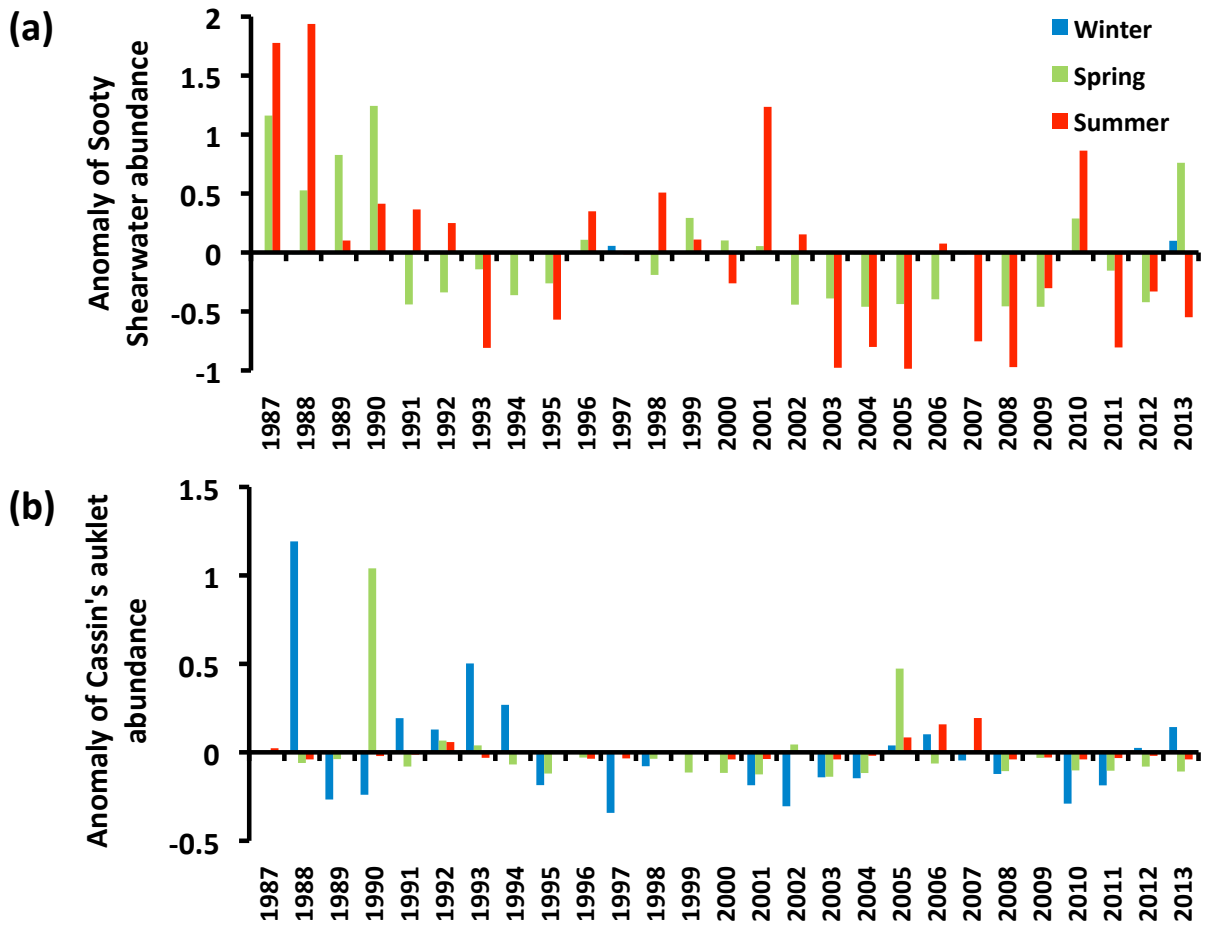

Figure 33. Patterns of change in the abundance (expressed as anomaly of density; long-term mean subtracted) of (a) sooty shearwater (*Puffinus griesus*) and (b) Cassin's auklet (*Ptychoramphus aleuticus*) over three seasons: winter, spring, and summer.

Seabirds integrate marine resources over local to large spatiotemporal scales (e.g., upwelling cells to ocean basins and synoptic to decadal time) such that their distribution and abundance at sea are excellent indicators of coupled climate-marine ecosystem variability. As part of the CalCOFI program, now supplemented by the CCE-LTER and SCCOOS programs, data on seasonal seabird distribution and abundance has been collected since spring 1987. Overall, total seabird abundance in the CalCOFI region has continued to display frequent negative seasonal and annual anomalies with only infrequent positive anomalies occurring once or twice a decade. Recently, Sydeman et al. (2014) attributed the 25-year decline in overall seabird abundance to declines in the availability of nearshore forage fish (primarily northern anchovy) and interannual variability in krill resources. Moreover, seabird species richness (total number of species recorded per survey) has also declined significantly (Sydeman et al. 2009). Together these frequent negative anomalies and the decline of total seabird abundance and species richness warrant further research to quantify the interactive effects of hydrographic and biological conditions on the viability of the seabird community within the CalCOFI region.

As examples of long-term variability of seabird abundance (indexed by density and expressed as numbers km^{-2}), we present data on two species, the sooty shearwater (*Puffinus griseus*; fig. 33a) and Cassin's auklet (*Ptychoramphus aleuticus*; fig. 33b). Sooty shearwaters are southern hemisphere migrants and are most abundant in the California Current during the spring and summer. Auklets are resident in the California Current yearround, but are most abundant in the CalCOFI region in winter. Shearwater density during spring has declined since surveys began in the late 1980s, with each successive peak in abundance (i.e., 1990, 2001, and 2010) lower than the preceding one. Shearwater abundance was lowest during the period 1993–95 and 2003–08. However, shearwaters exhibited a strong positive anomaly during spring 2013, which was similar in magnitude to the peaks recorded earlier in the history of this survey. The abundance of auklets also fluctuates, with no overall change registered since 1998–99. Recent peaks in auklet abundance were due to unusual increases in density

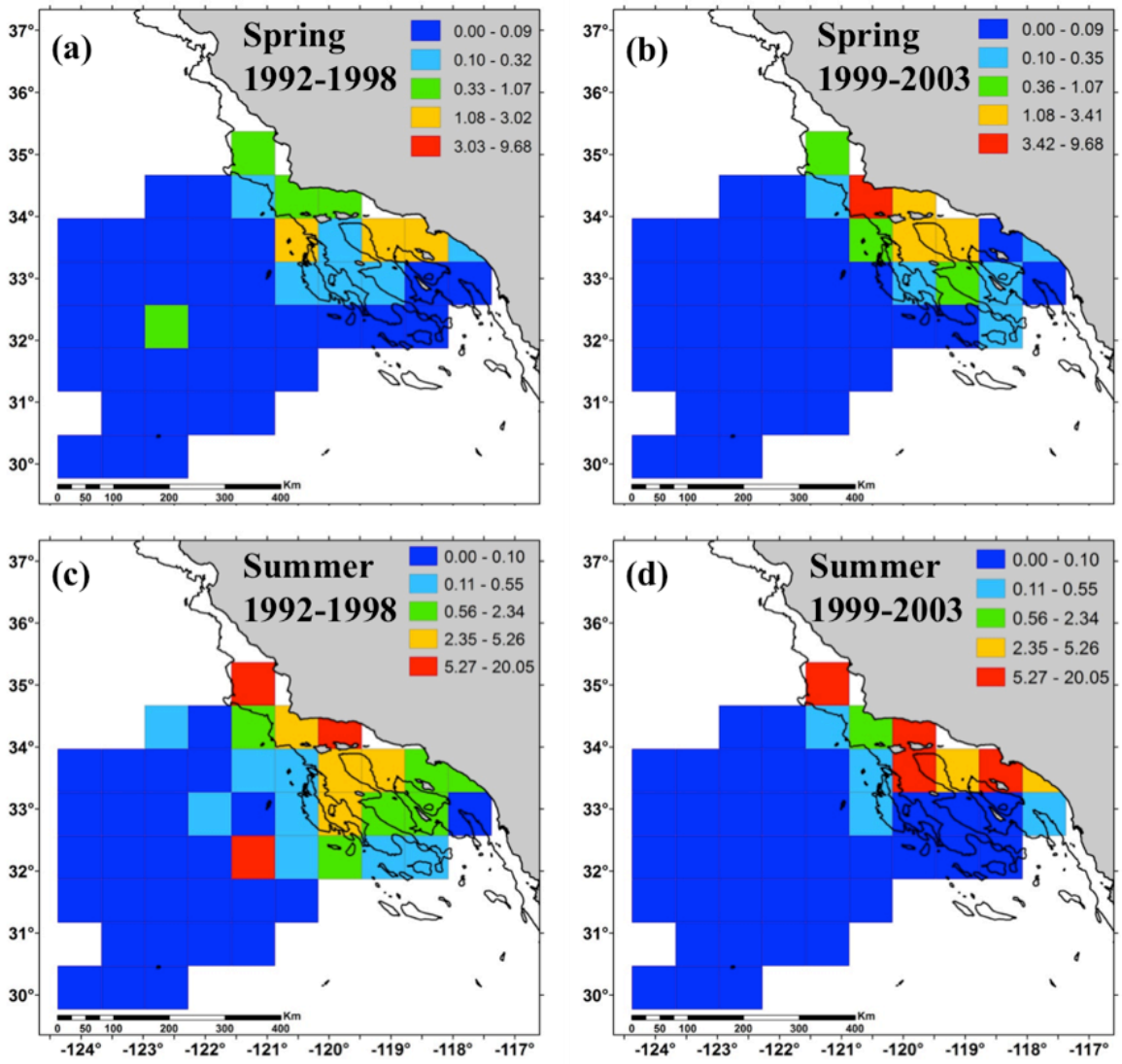

Figure 34. Spatial mean abundance of sooty shearwater from spring and summer CalCOFI surveys during two contrasting periods of El Niño and La Niña: 1992–98 and 1999–2003.

in spring 2005 and summer 2005–07 (related to colony abandonment from the Farallon Islands; Sydeman et al. 2006). However, auklets exhibited a positive anomaly during winter 2013 (largest positive anomaly since 2006) that is similar in magnitude to their anomalies recorded during winter 1991 and 1992.

Mapping seabird distributions in the CalCOFI region reveals that seabird community structure varies annually according to warm and a cool ocean temperatures, with more subtropical species recorded during anomalously warm years (Hyrenbach and Veit 2003) and "hotspots" of abundance associated with Point Conception (Yen et al. 2006). For example, species such as Cook's petrel (*Pterodroma cookii*), black storm petrel (*Oceanodroma melania*) and black-vented shearwater (*Puffinus opisthomelas*) are relatively more abundant during El Niño years. Moreover, Hyrenbach and Veit (2003) found that some species with a warm-water affinity increased before the event, while those with a cold-water affinity decreased, suggesting leading indicators of impending El Niño conditions. As examples of these temporal changes in seabird distribution, spatial climatologies of sooty shearwater abundance during two different periods are provided: 1992–98, a prolonged warm-water period associated with the strong El Niño events of 1992–93 (Trenberth and Hoar 1996) and 1997–98; and 1999–2003, a period dominated by La Niña cold-water conditions (Bograd and Lynn 2001; Yen et al. 2006). The spatial mean abundance of shearwaters during spring and summer from these two periods indicate that shearwaters are more abundant and clustered in the coastal domain of the Santa Barbara Basin during the cool period (1999–2003) in comparison to the warm period (1992–98) when they are generally less abundant and more dispersed (fig. 34).

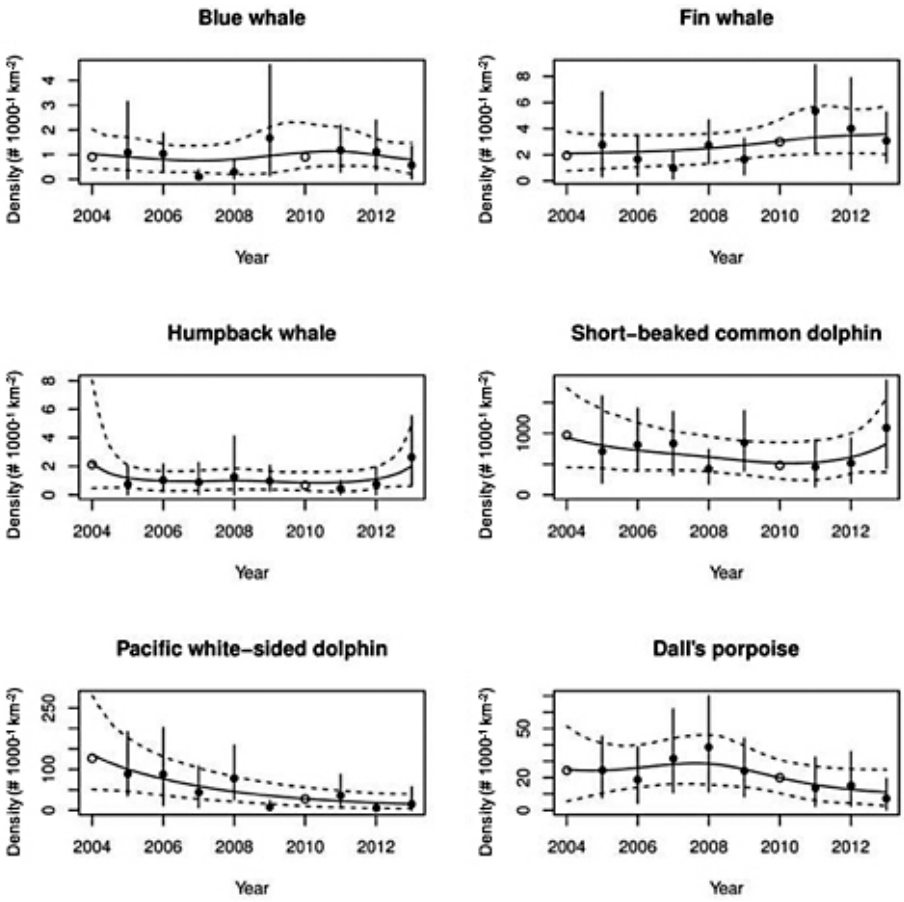

Figure 35. Annual and long-term trend in density by cetacean species. Dots are the mean over seasons of the annual density estimates by year and vertical lines show 95% bootstrap confidence intervals, except for 2004 and 2010 where the dots are the mean of the seasonal estimates where available and the predicted values from the GAM in seasons where no survey was performed. Solid line represents the predicted long-term trend from the GAM and dashed lines represent lower and upper 95% confidence intervals.

If indeed a strong El Niño does impacts the California Current during 2014–15, we can expect lower seabird abundance and biomass, as well as an influx of the usual El Niño visitor species. In addition, we also predict that the number and intensity of seabird-forage hotspots would be far less and clustered in coastal upwelling habitats during the El Niño event. In summary, we expect seabird abundance and species occurrence patterns to provide early-warning indications of ecosystem variability resulting from the impending El Niño event.

Cetacean Density on the Southern CalCOFI Lines from 2004–13

Density estimates for the six most common cetacean species off southern California in 2013 were compared to long-term averages from 2004–12.[4] Despite higher point estimates for five of the six species in 2013, z-tests indicated these differences were not significantly different from the estimates reported for the pooled 2004–12 surveys (fig. 35). The relatively small sample sizes and associated large variances from a single year preclude a more informative statistical comparison. Overall annual trend analysis indicated that there were no significant changes in blue whale, fin whale, humpback whale, short-beaked common dolphin, or Dall's porpoise densities across the ten-year study period; however, Pacific white-sided dolphins exhibited a significant decrease in density with a mean annual population decrease of 22.5% (95% CI = –34.52% – –9.43%) (fig. 35).

California Sea Lions at San Miguel Island, California

California sea lions (*Zalophus californianus*) are permanent residents of the CCS, breeding in the California Channel Islands and feeding throughout the CCS in coastal and offshore habitats. They are also sensitive to changes in the CCS on different temporal and spatial scales and so provide a good indicator species for the status of the CCS at the upper trophic level (Melin et al.

[4]A detailed description of the field and analytical methods utilized for the analysis presented here can be found in: Campbell, G. S., L. Thomas, K. Whitaker, A. Douglas, J. Calambokidis, and J. A. Hildebrand. In Revision. Interannual and seasonal trends in cetacean distribution, density, and abundance in waters off southern California. DSRII Special CalCOFI Issue.

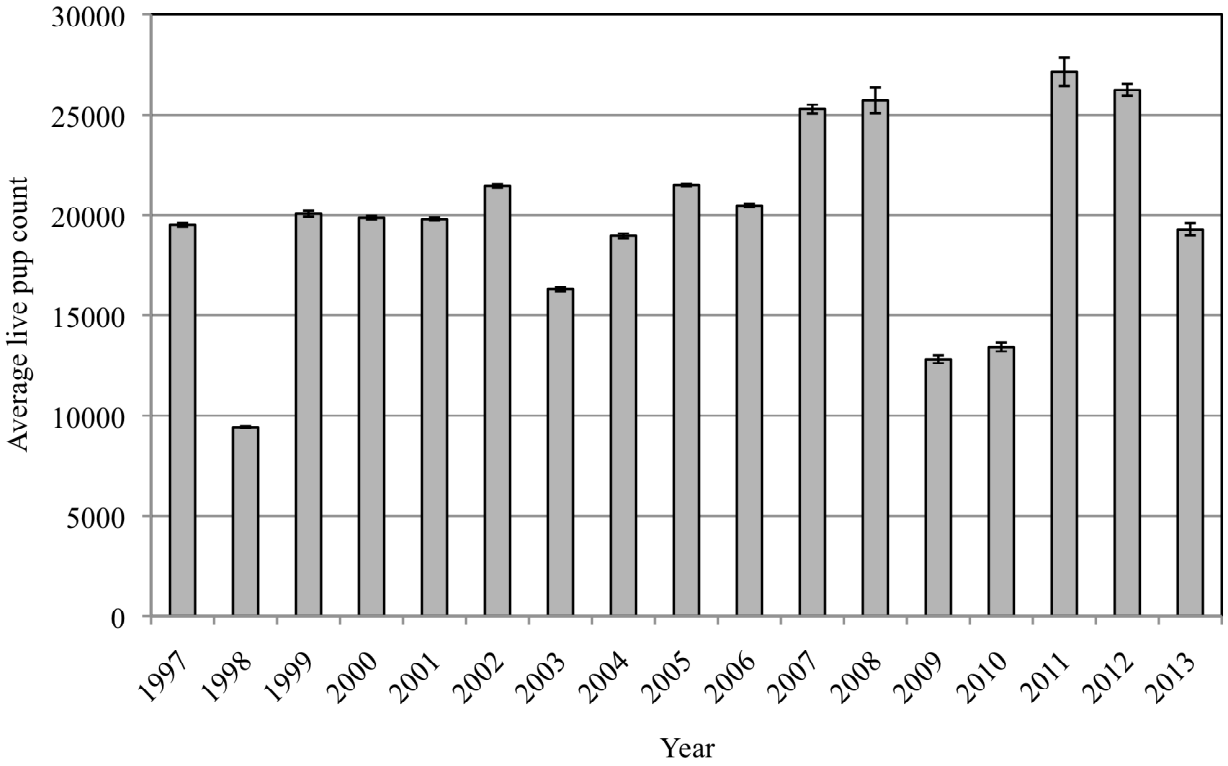

Figure 36. The average number of live California sea lion pups counted at San Miguel Island, California, 1997–2013 in late July when surviving pups were about 6 weeks old. Error bars are ±1 standard error.

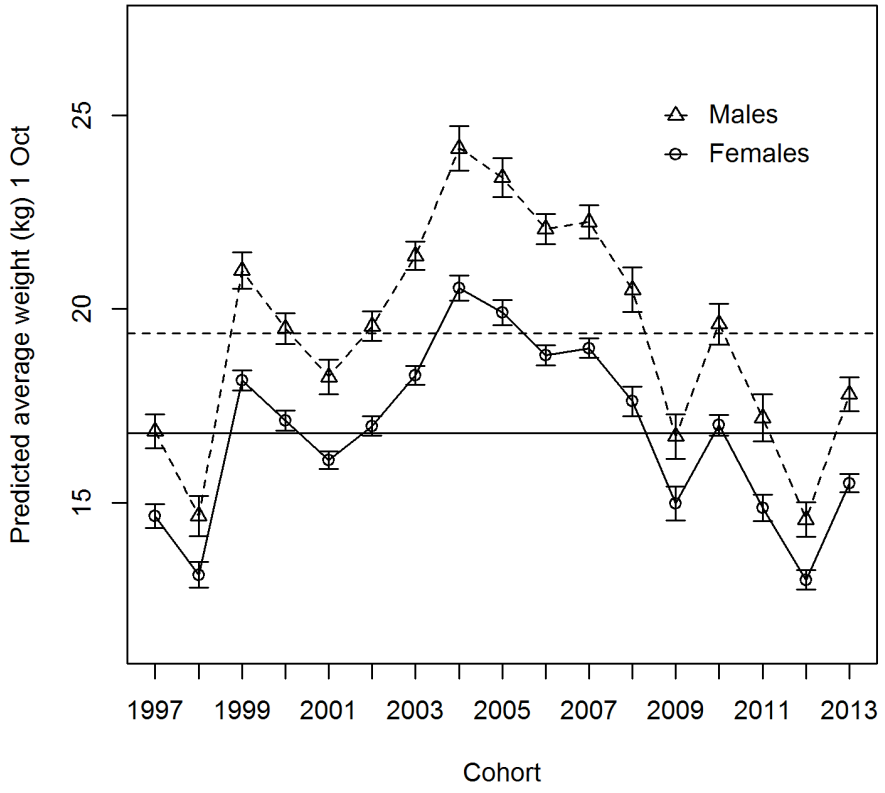

Figure 37. Predicted average weights of 4 month old female (open circle) and male (open triangle) California sea lion pups at San Miguel Island, California, 1997–2013 and long-term average between 1975 and 2013 for females (solid line) and males (dashed line). Error bars are ±1 standard error.

2012). San Miguel Island, California (34.03°N, 120.4°W) is one of the largest colonies of California sea lions, representing about 45% of the US breeding population. As such, it is a useful colony to measure trends and population responses to changes in the marine environment. We used the number of pups alive at the time of the live pup census conducted in late July and the average weights of pups at 4 months and 7 months of age between 1997 and 2013 as indices of the population response to annual conditions in the CCS. The number of live pups in late July represents the number of pups that survived from birth to about 6 weeks of age. Live pups were counted after all pups were born (between 20–30 July) each year. A mean of the number of live pups was calculated from the total number of live pups counted by each observer. Each year, between 200 and 500 pups were weighed when about 4 months old. Pups were sexed, weighed, tagged, branded, and released. Up to 60 pups were captured in February and weighed and measured at 7 months of age. Of the 60 pups captured in February, up to 30 pups were branded and provided a longitudinal data set for estimating a daily growth rate between 4 months and 7 months old. We used a linear mixed-effects model fit by REML in R to predict average weights on 1 October and 1 February in each year because the weighing dates were not the same among years. The model contained random effects with a sex and days interaction (days = the number of days between weighing and 1 October or 1 February) that allowed the growth rate to vary by sex and year, and a full interaction fixed effects of sex and days. The average weights between 1997 and 2013 were compared to the long-term average for the average pup weights between 1975 and 2013.

In March 2013, an Unusual Mortality Event (UME) was declared for California sea lions in southern California (http://www.nmfs.noaa.gov/pr/health/mmume/californiasealions2013.htm) in response to unprecedented numbers of young pups from the 2012 cohort stranding along the coast between January and March and poor condition of pups at San Miguel Island and other rookeries during the winter (Wells et al. 2013). By the onset of the California sea lion reproductive season in June 2013, most of the population indices for California sea lions at San Miguel Island showed signs of improvement. Although the average number of live pups counted at San Miguel Island in July 2013 declined 27% from 2012 (fig. 36), the pup growth indices indicated that the condition of dependent pups from the 2013 cohort had improved considerably from 2012. However, pup weights at 4 months of age (fig. 37), 7 months of age (fig. 38) and growth rates to 7 months of age (fig. 39) still remained below the long-term average.

The decline in pup production reflects the inability of adult females to support pregnancies during the winter and spring of 2013 and coincides with a reduced availability of Pacific sardine and northern anchovy in the spring of 2013 as indicated by surveys in central California in spring 2013 (Wells et al. 2013). The improved condition of pups in 2013 suggests that foraging conditions improved for lactating females during the period of pup dependence.

DISCUSSION

During 2013, upwelling started early and was relatively strong during the entire summer, leading to one of the highest cumulative upwelling indices on record for much of the coastal CCS (fig. 3). The enhanced upwelling was most evident from central to mid-California, with decreased enhancement in northern California and Oregon. As a result, surface temperatures in most areas during spring and early summer were low and chlorophyll *a* was high, although not as high as expected in northern California and Oregon. Both northern California and Oregon observed high numbers of "northern copepods"—an indicator of good feeding conditions for higher trophic levels, particularly fish, since this copepod species assemblage typically has high levels of lipids (Peterson and Keister 2003; Hoof and Peterson 2006; Peterson 2009).

Based on the strong upwelling, 2013 was expected to be a highly productive year, particularly for coastal species. The strong upwelling in the winter of 2013 was due to a strong north Pacific high (Schroeder et al. 2013), which results in high production, especially in central California (Black et al. 2010; Black et al. 2011; Garcia et al. 2014). Off Oregon, larval rockfish were found in higher than average numbers during the summer, whereas larval northern anchovy were found at low concentrations; within the central CCS, strong upwelling may reduce anchovy density (Santora et al. 2014). Also, juvenile coho salmon were found at high numbers during summer 2013. A PCA of pelagic fish species found that off Oregon, 2013 was similar to 2006, 2008, and 2012. On the central California coast, juvenile rockfish were found at very high abundances, along with market squid and krill, and a moderately high abundance of Pacific hake. These findings are consistent with 2013 being a year that favored species that respond to high transport and coastal upwelling conditions in the winter and spring (Black et al. 2011; Santora et al. 2014).

In general, the response of seabirds within the CCS to this heightened coastal productivity was also positive. Murres in northern California fledged an above average number of young in 2013. Breeding at Southeast Farallon Island was also high for all species examined there, with Cassin's auklets having an exceptional year. The bird species examined all tend to feed on prey that responds

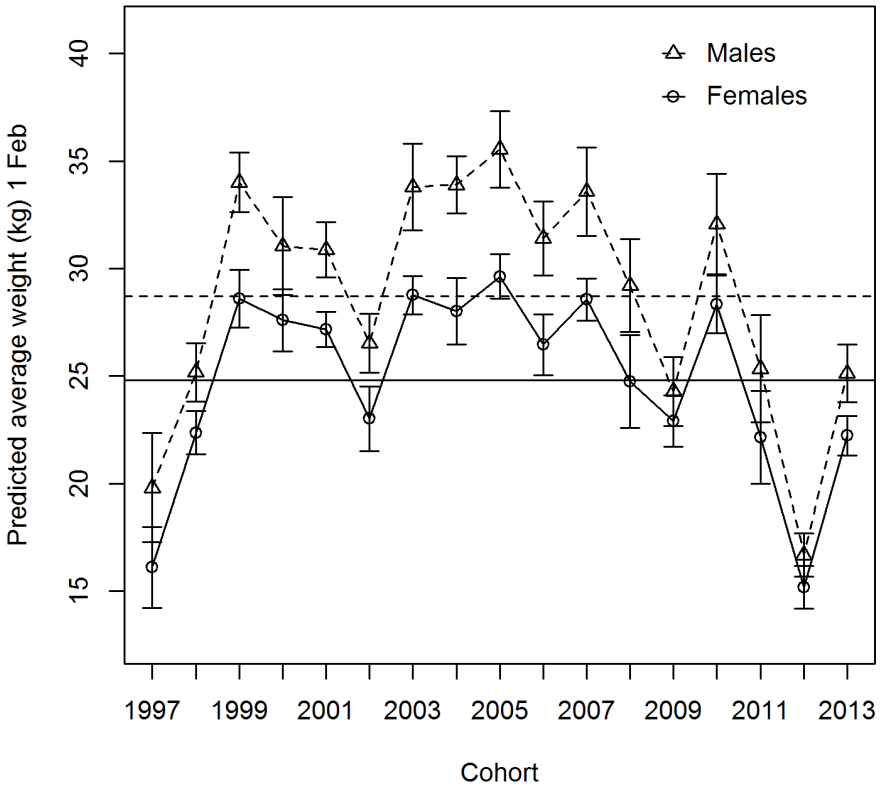

Figure 38. Predicted average weights of 7 month old female (open circle) and male (open triangle) California sea lion pups at San Miguel Island, California, 1997–2013 and long-term average between 1975 and 2013 for females (solid line) and males (dashed line). Error bars are ±1 standard error.

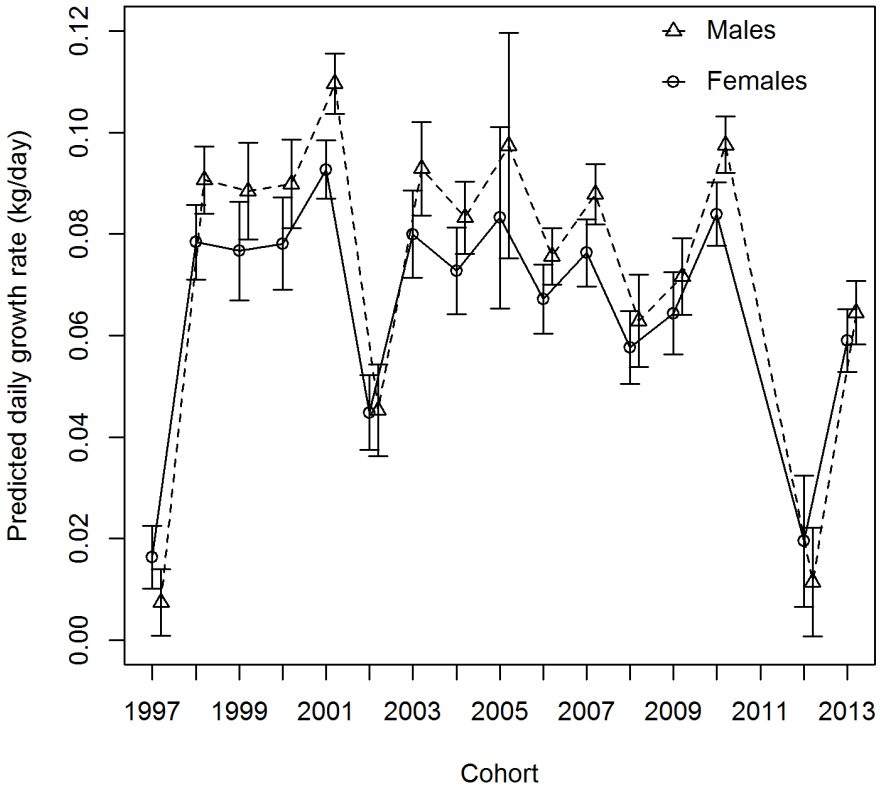

Figure 39. Predicted average daily growth rate of female (open circle) and male (open triangle) California sea lion pups between 4 and 7 months old at San Miguel Island, California, 1997–2013. Error bars are ±1 standard error.

well to upwelling; in these cases, the high numbers of juvenile rockfish and euphausiids that responded to the increased upwelling during 2013 (Ainley et al. 1995; Wells et al. 2013; Santora et al. 2014). Farther north, in Oregon, the murres at Yaquina head did not show a positive response in 2013, however, this was likely due to increased predation on the chicks and eggs. Within the CalCOFI region, sooty shearwater abundance was high in spring, but was low during summer 2013; the majority of the CalCOFI region was not as heavily influenced by the strong 2013 upwelling that occurred primarily along central California.

The previous year's SOTCC annual report (Wells et al. 2013) speculated on the potential effects of the strong winds that occurred early in 2013 on the overall productivity and structure of the ecosystem. Specifically, such anomalously strong winds could lead to increased diffusion of nutrients and phytoplankton away from the coast, and concomitant changes in the upwelling reliant species. Within the CalCOFI region, where there were subsurface measurements of nutrients, this was clearly not the case; 2013 saw high levels of nitrate, particularly during the spring (April) cruise (fig. S7). Primary production and chlorophyll *a* were also generally high throughout the CalCOFI region for most of 2013 (fig. S8). Chlorophyll *a* levels were also high along coastal central California, as evidenced by the observations from Monterey Bay (fig. 14). In a detailed spatial analysis of chlorophyll *a* long-term trends, 2013 also showed relatively high levels of chlorophyll *a* compared to the long-term mean for most regions examined (fig. 9). Chlorophyll *a* levels sampled off of Oregon were also high throughout 2013 (fig. 11). The Trinidad Head line was the one exception to this, with relatively low chlorophyll *a* throughout 2013, as compared to previous years (fig. 12). Thus productivity, at least as evidenced by chlorophyll *a* biomass, does not seem to have been negatively impacted by "too much upwelling," except perhaps at a few limited locations. This is in contrast to another recent high upwelling year, 1999, in which chlorophyll *a* concentrations were observed to be high nearly 50 km offshore rather than next to the coast, consistent with the offshore position of the upwelling front (Schwing et al. 2000). However, as correctly predicted, the strong upwelling and resulting high coastal productivity did favor species which rely on this type of structure; northern copepod species saw increased abundances to the north, and within the south, total zooplankton volumes were high. Species such as juvenile rockfish (*Sebastes* spp.) and market squid thrived, whereas sardine and anchovy abundances were very low.

In the spring and early summer of 2014 the CCS transitioned away from the cool, strong upwelling conditions of 2013, marking a significant change in the state of the California Current from the past few years. As of August 2014, most basin-scale indices suggest that 2014 is transitioning to a moderate El Niño state. The ENSO-MEI, PDO, and NPGO all changed sign during the winter of 2013–14 (table 1, fig. S1). SST was anomalously high throughout most of the CCS during spring and summer 2014, with springtime chlorophyll *a* levels anomalously low in nearly all locations, except a few spots along the central coast. Surface temperatures measured from coastal buoys were also high during the spring of 2014, except for the northernmost stations. Unlike SST and chlorophyll *a*, several indices remain more near a "neutral state" similar to the long-term monthly or seasonal climatological means. Upwelling anomaly was neutral or only slightly negative throughout most of the coastal region during the spring and early summer (fig. 2). The cumulative upwelling index was also near long-term seasonal averages for most locations (fig. 3). Biomass of northern copepods off Oregon remained relatively high through early summer of 2014 (fig. 11), which is counter-indicative of an El Niño state (Peterson et al. 2002; Hoof and Peterson 2006). Within the CalCOFI region, spring 2014 yielded very few sardine eggs or larvae, and also very low numbers of adults, although the distribution of adults was likely very patchy, confounding an interpretation of abundance (fig. 26). Sardine and anchovy abundance was also low along the central coast (fig. 22), similar to conditions found during past El Niños (McClatchie 2014). Conditions in the Equatorial Pacific signify a developing El Niño but its current impact on environmental conditions in the CCS due to atmospheric teleconnections is not so pronounced (Schwing et al. 2002a; Schwing et al. 2002b; Schwing et al. 2005). So far, the effects seem to be more to the very north and south ends of the CCS, with a much more minor impact to the central coast area. Upwelling and chlorophyll *a* levels are still near the climatological means for the mid to central California coast. Catches of rockfish, market squid, pacific sanddab, and euphausiids were also high along the central and southern California coast during summer 2014 (fig. 22). The effects of the looming El Niño also seem to have impacted a larger total area of the CCS during the winter of 2013–14, as compared to the late spring of 2014, which saw a moderate amount of upwelling in certain locations. The winter of 2013–14 saw some of the larger anomalous El Niño-type values throughout the region, which corresponded to warm SST in the central equatorial region and lead to the prediction of an El Niño event occurring in 2014 (Ludescher et al. 2014).

Comparing the conditions leading up to this point within the CCS with previous time periods leading up

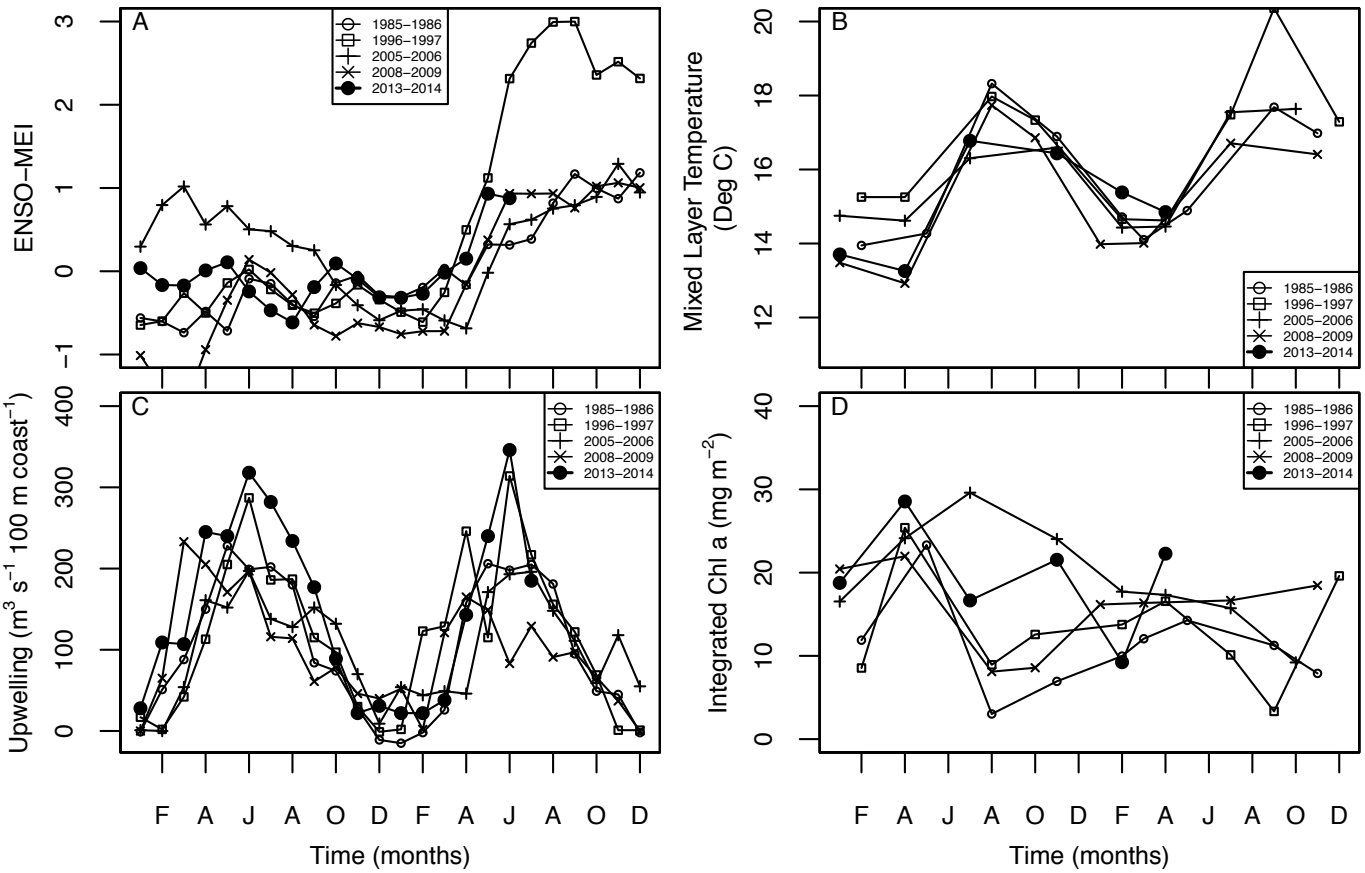

Figure 40. Selected indicators for Jan 2013 to July 2014 by month versus similar time periods leading up to several past El Niño events; a) MEI- ENSO index, b) Average mixed-layer temperature within the CalCOFI grid, c) Average upwelling index from 36N, 122W, and d) Chlorophyll *a* integrated within the mixed layer from the CalCOFI grid.

to other El Niños suggests this will be only a moderate event (fig. 40), if it does occur (as of Oct 2014, NOAA's National Weather Service predicts a weak El Niño to begin in Nov–Dec and last until spring 2015; http://www.elnino.noaa.gov). The ENSO-MEI index for Jan 2013–July 2014 was similar to the more moderate El Niños, with a notable drop off for June, and unlike the strong 1996–98 El Niño (fig. 40a). Average mixed-layer temperature throughout the CalCOFI region was also most similar to the more moderate El Niño of 2005–06 during this lead-in period than the other El Niños compared (fig. 40b). Upwelling during this lead-in period was also similar to previous El Niños, although higher for certain months than several other comparable El Niños (fig. 40c). Chlorophyll *a* also appears to have been higher during this lead-in period than the other El Niños (except the 05–06 time period, and February 2014; this latter cruise only covered the southern portion of the grid, thus this average is artificially low for that month). Unlike these past El Niños, we know that the lead-in year, 2013, was a year of generally strong upwelling, with generally enhanced biological response. What is unclear is how much this longer-term El Niño "preconditioning" could be affecting the evolution of the impacts of the predicted, apparently mild, El Niño on the CCS.

Already it is clear that as of the end of August 2014, at least some portions of the central, coastal CCS are not as impacted—upwelling remains near climatological levels and chlorophyl *a* remains high. However, the more detailed spatially explicit analysis of temperature and chlorophyll *a* suggests that the majority of the CCS is both warm and low in chlorophyll *a* (figs. 7–9). If this spatial trend continues—mild El Niño conditions for the northern, most southern, and offshore portions of the CCS, with moderate upwelling along the central coast—then it may be that 2014 will be a year with a very patchy distribution in production, and fairly different overall from 2013. Indeed, the most recent view of chlorophyll *a* anomaly for July 2014 shows a very patchy distribution of both low and high chlorophyll *a* regions spread throughout the nearshore region, with a pattern markedly different from only a few months ago (fig. 6). How this spatial and temporal patchiness in upwelling, chlorophyll *a*, and presumably productivity will affect the evolution of the ecosystem during

2014 remains to be seen, but may result in an interesting mix of El Niño responsive species in the most southern, northern, and offshore regions, with nearshore patches of upwelling-dominant species. Superimposed on these conditions, recent analysis of satellite SST and wind data shows that there has been extensive, possibly non-El Niño-related warming to three major areas within the Northeast Pacific: the Bering Sea; the Gulf of Alaska; and most recently, offshore of southern California (Milstein et al. NOAA-Technical Report, 2014, http://www.nwfsc.noaa.gov/news/features/food_chain/index.cfm). Although it is unclear exactly how the looming El Niño will interact with these warm pools, the likely result will be even more warming and stronger El Niño-like conditions than expected from a moderate El Niño alone; such conditions are generally unfavorable to many key fisheries species.

ACKNOWLEDGEMENTS

Andrew W. Leising was partially funded through NOAA's Fisheries and the Environment (FATE) program. Ichthyoplankton collections off the Oregon coast were supported in part by NOAA's Stock Assessment Improvement Plan (SAIP) and Fisheries and the Environment (FATE) programs, as well as from a grant through the Bonneville Power Administration (BPA). Financial support was provided by the NASA Ocean Biology and Biogeochemistry Program Grants NNX-09AT01G (M. K.), National Science Foundation (Grant OCE-1026607 to the CCE LTER Program). Satellite data were provided by the NASA Ocean Color Processing Group and ESA MERIS team. We thank the CalCOFI and CCE-LTER programs, NOAA SWFSC survey, Monterey Bay Aquarium Research Institute and Pacific Coastal Ocean Observing System for in situ data. R. DeLong, J. Harris, J. Laake, A. Orr and many field assistants participated in the data collection and summaries. Funding was provided by the National Marine Fisheries Service. Research was conducted under NMFS Permit 16087 issued to the National Marine Mammal Laboratory.

LITERATURE CITED

Ainley, D. G., W. J. Sydeman, and J. Norton. 1995. Upper trophic level predators indicate interannual negative and positive anomalies in the California Current food web. Marine Ecology Progress Series 118:69–79.

Auth, T. D. 2011. Analysis of the spring-fall epipelagic ichthyoplankton community in the northern California Current in 2004–09 and its relation to environmental factors. Calif. Coop. Oceanic. Fish. Invest. Rep. 52:148–167.

Bakun, A. 1973. Coastal upwelling indices, west coast of North America, 1946–71. U.S. Dep. Commer., NOAA Tech. Rep., NMFS SSRF-671, 103 p.

Bjerknes, J. 1966. A possible response of the atmospheric Hadley circulation to equatorial anomalies of ocean temperature. Tellus, 18:820–829. doi: 10.1111/j.2153–3490.1966.tb00303.x.

Bjorkstedt, E., R. Goericke, S. McClatchie, E. Weber, W. Watson, N. Lo, B. Peterson, B. Emmett, R. Brodeur, J. Peterson, M. Litz, J. Gomez-Valdez, G. Gaxiola-Castro, B. Lavaniegos, F. Chavez, C. A. Collins, J. Field, K. Sakuma, P. Warzybok, R. Bradley, J. Jahncke, S. Bograd, F. Schwing, G. S. Campbell, J. Hildebrand, W. Sydeman, S. Thompson, J. Largier, C. Halle, S.Y. Kim, and J. Abell. 2012. State of the California Current 2010–11: Regional Variable Responses to a Strong (But Fleeting?) La Niña. California Cooperative Oceanic Fisheries Investigations Report 52:36–68.

Black, B. A., I. D. Schroeder, W. J. Sydeman, S. J. Bograd, and P. W. Lawson. 2010. Wintertime ocean conditions synchronize rockfish growth and seabird reproduction in the central California Current ecosystem. Canadian Journal of Fisheries and Aquatic Sciences 67:1149–1158.

Black, B. A., I. D. Schroeder, W. J. Sydeman, S. J. Bograd, B. K. Wells, and F. B. Schwing. 2011. Winter and summer upwelling modes and their biological importance in the California Current Ecosystem. Global Change Biology.

Bograd, S. J., and R. J. Lynn. 2001. Physical-biological coupling in the California Current during the 1997–99 El Niño-La Niña cycle. Geophysical Research Letters 28: 275–278.

Bograd, S. J., I. Schroeder, N. Sarkar, X. M. Qiu, W. J. Sydeman, and F. B. Schwing. 2009. Phenology of coastal upwelling in the California Current. Geophysical Research Letters 36:doi 10.1029/2008gl035933.

Brodeur, R. D., J. P. Fisher, R. L. Emmett, C. A. Morgan, and E. Casillas. 2005. Species composition and community structure of pelagic nekton off Oregon and Washington under variable oceanographic conditions. Mar. Ecol. Prog. Ser. 298:41–57.

Daly, E. A., T. D. Auth, R. D. Brodeur, and W. T. Peterson. 2013. Winter ichthyoplankton biomass as a predictor of early summer prey fields and survival of juvenile salmon. Mar. Ecol. Prog. Ser. doi:10.3359/meps10320.

Di Lorenzo, E., N. Schneider, K. M. Cobb, P. J. S. Franks, K. Chhak, A. J. Miller, J. C. McWilliams, S. J. Bograd, H. Arango, E. Curchitser, T. M. Powell, and P. Riviere. 2008. North Pacific Gyre Oscillation links ocean climate and ecosystem change. Geophysical Research Letters 35:doi 10.1029/2007gl032838.

Gladics, A. J., R. M. Suryan, J. K. Parrish, C. A. Horton, E. A. Daly, and W. T. Peterson. In review. Environmental drivers and reproductive consequences of variation in the diet of a marine predator. Journal of Marine Systems.

Hooff, R. C., and W. T. Peterson. 2006. Copepod biodiversity as an indicator of changes in ocean and climate conditions of the northern California current ecosystem. Limnology and Oceanography 51(6).

Horton, C. A. 2014. Top-down influences of Bald Eagles on Common Murre populations in Oregon. MS thesis, Oregon State University.

Horton, C. A., and R. M. Suryan. 2012. Brown Pelicans: A new disturbance source to breeding Common Murres in Oregon? Oregon Birds 38:84–88.

Hyrenbach, K. D., and R. R. Veit. 2003. Ocean warming and seabird communities of the Southern California Current System (1987–98): response at multiple temporal scales. Deep-Sea Research Part II 50:2537–2565.

Kahru, M., and B. G. Mitchell. 2001. Seasonal and non-seasonal variability of satellite-derived chlorophyll and CDOM concentration in the California Current, *J. Geophys. Res*, 106(C2): 2517–2529.

Kahru, M., and B. G. Mitchell. 2002. Influence of the El Niño–La Niña cycle on satellite-derived primary production in the California Current, *Geophys. Res. Let.*, 29(17), doi: 10.1029/2002GL014963.

Kahru, M., R. M. Kudela, M. Manzano-Sarabia, and B. G. Mitchell. 2012. Trends in the surface chlorophyll of the California Current: Merging data from multiple ocean color satellites, *Deep-Sea Research* II, 77–80, 89–98.

Ludescher, J., A. Gozolchiani, M. I. Bogachev, A. Bunde, S. Havlin, and H. J. Schellnhuber. 2014. Very early warning of next El Niño. Proceedings of the National Academy of Sciences 111:2064–2066.

Lynn, R. J., J. J. Simpson. 1987. The California Current system: The seasonal variability of its physical characteristics. *J. Geophys. Res.*, 92, 12,947–12,966.

McClatchie, S. Regional fisheries oceanography of the California Current System: the CalCOFI program. Springer. 235pp. ISBN 978-94-007-7222-9, 2014.

McCune, B., and M. J. Mefford. 2011. PC-ORD. Multivariate Analysis of Ecological Data. Version 6. MjM Software, Gleneden Beach, OR, USA.

Melin, S. R., A. J. Orr, J. D. Harris, J. L. Laake, R. L. DeLong, F. M. D. Gulland, and S. Stoudt. 2010. Unprecedented mortality of California sea lion pups associated with anomalous oceanographic conditions along the central California coast in 2009. California Cooperative Ocean and Fisheries Investigations Reports 51: 182–194.

Melin, S. R., A. J. Orr, J. D. Harris, J. L. Laake, and R. L. DeLong. 2012. California sea lions: An indicator for integrated ecosystem assessment of the California Current System. California Cooperative Ocean and Fisheries Investigations Reports 53:140–152.

Peterson, W. T., and J. E. Keister. 2003. Interannual variability in copepod community composition at a coastal station in the northern California

Current: a multivariate approach. Deep Sea Research Part II: Topical Studies in Oceanography 50:2499–2517.

Peterson, W. T., J. E. Keister, and L. R. Feinberg. 2002. The effects of the 1997–99 El Niño/La Niña events on hydrography and zooplankton off the central Oregon coast. Progress In Oceanography 54:381–398.

Ralston, S., and I. J. Stewart. 2013. Anomalous distributions of pelagic juvenile rockfish on the U.S. west coast in 2005 and 2006. CalCOFI Reports 54:155–166.

Ralston, S., K. M. Sakuma, and J. C. Field. 2013. Interannual variation in pelagic juvenile rockfish (*Sebastes* spp.) abundance—going with the flow. Fisheries Oceanography 22:4: 288–308.

Ralston, S., J.C. Field, and K. M. Sakuma. 2014. Long-term variation in a central California pelagic forage assemblage. Journal of Marine Systems (in press). http://dx.doi.org/10.1016/j.jmarsys.2014.06.013.

Santora, J. A., I. D. Schroeder, J. C. Field, B. K. Wells, and W. J. Sydeman. 2014. Spatio-temporal dynamics of ocean conditions and forage taxa reveals regional structuring of seabird-prey relationships. Ecological Applications In Press.

Schroeder, I. D., B. A. Black, W. J. Sydeman, S. J. Bograd, E. L. Hazen, J. A. Santora, and B. K. Wells. 2013. The North Pacific High and wintertime pre-conditioning of California current productivity. Geophysical Research Letters 40.

Schwing, F. B., M. O'Farrell, J. M. Steger, and K. Baltz. 1996. Coastal upwelling indices, West Coast of North America, 1946–1995, NOAA Tech. Memo., NOAA-TM-NMFS-SWFSC-231, 144 pp.

Schwing, F. B., C. S. Moore, S. Ralston, and K. M. Sakuma. 2000. Record coastal upwelling in the California Current in 1999. *Reports of California Cooperative Oceanic Fisheries Investigations*, 41, 148–160.

Schwing, F. B., T. Murphree, L. deWitt, and P. M. Green. 2002a. The evolution of oceanic and atmospheric anomalies in the northeast Pacific during the El Niño and La Niña events of 1995–2001. Progress In Oceanography 54:459–491.

Schwing, F. B., T. Murphree, and P. M. Green. 2002b. The Northern Oscillation Index (NOI): a new climate index for the northeast Pacific. Progress In Oceanography 53:115–139.

Schwing, F. B, D. M. Palacios, and S. J. Bograd. 2005. El Niño Impacts of the California Current Ecosystem. U.S. CLIVAR Variations 3(2):5–8.

Sydeman, W. J., R. W. Bradley, P. Warzybok, C. L. Abraham, J. Jahncke, K. D. Hyrenbach, V. Kousky, J. M. Hipfner, and M. D. Ohman. 2006. Planktivorous auklet Ptychoramphus aleuticus responses to ocean climate, 2005: Unusual atmospheric blocking? Geophysical Research Letters 33:L22S09.

Sydeman, W. J., K. L. Mills, J. A. Santora, S. A. Thompson, D. F. Bertram, K. H. Morgan, B. K. Wells, J. M. Hipfner, and S. G. Wolf. 2009. Seabirds and climate in the California Current—A synthesis of change. CalCOFI Report 50:82–104.

Sydeman, W. J., S. A. Thompson, J. A. Santora, J. A. Koslow, R. Goericke, and M. D. Ohman. 2014. Climate-ecosystem change off southern California: time-dependent seabird predator-prey numerical responses. Deep-Sea Research II.

Thompson, A. R., T. D. Auth, R. D. Brodeur, N. M. Bowlin, and W. Watson. 2014. Dynamics of larval fish assemblages in the California Current System: a comparative study between Oregon and southern California. Mar. Ecol. Prog. Ser. 506:193–212

Trenberth, K. E., and J.W. Hurrell. 1994. Decadal atmosphere-ocean variations in the Pacific. Clim. Dyn. 9, 303–319.

Trenberth, K. E., and T. J. Hoar. 1996. The 1990–95 El Niño–Southern Oscillation event: Longest on record. Geophysical Research Letters, 23: 57–60.

Veit, R. R., P. Pyle, and J. A. McGowan. 1996. Ocean warming and long-term change in pelagic bird abundance within the California Current system. Marine Ecology Progress Series 139:11–18.

Wells, B. K., and 47 other authors. 2013. State of the California Current 2012–13: No such thing as an "average" year. CalCOFI Reports 54: 37–71.

Wolter, K., and M. S. Timlin. 1998. Measuring the strength of ENSO events—how does 1997/98 rank? Weather 53:315–324.

Yen, P. P. W., W. J. Sydeman, S. J. Bograd, and K. D. Hyrenbach. 2006. Springtime distributions of migratory marine birds in the southern California Current: oceanic eddy associations and coastal habitat hotspots over 17 years. Deep-Sea Research II 53: 399–418.